

RESEARCH PAPER



Synthesis and structure–activity relationships of pyrazole-based inhibitors of meprin α and β

Kathrin Tan^a , Christian Jäger^b , Stefanie Geissler^a , Dagmar Schlenzig^a , Mirko Buchholz^{a*}  and Daniel Ramsbeck^a 

^aDepartment of Drug Design and Target Validation MWT, Fraunhofer Institute for Cell Therapy and Immunology IZI, Biocenter, Halle (Saale), Germany; ^bVivoryon Therapeutics N.V., Halle (Saale), Germany

ABSTRACT

Targeting metalloproteinases has been in the focus of drug design for a long time. However, meprin α and β emerged as potential drug targets just recently and are linked to several diseases with different pathological background. Nevertheless, the validation of meprins as suitable drug targets still requires highly potent and selective inhibitors as chemical probes to elucidate their role in pathophysiology. Albeit highly selective inhibitors of meprin β have already been reported, only inhibitors of meprin α with modest activity or selectivity are known. Starting from recently reported heteroaromatic scaffolds, the aim of this study was the optimisation of meprin α and/or meprin β inhibition while keeping the favourable off-target inhibition profile over other metalloproteases. We report potent pan-meprin inhibitors as well as highly active inhibitors of meprin α with superior selectivity over meprin β . The latter are suitable to serve as chemical probes and enable further target validation.

ARTICLE HISTORY

Received 30 September 2022
Revised 30 December 2022
Accepted 2 January 2023

KEYWORDS



Meprin; metalloprotease; hydroxamate; inhibitor; pyrazole

Introduction


Proteases are involved in numerous processes that regulate the proper function of organisms. An impaired function of proteases or a dysregulation of proteolytic networks could lead to the development of diseases. Thus, proteases have always been important and promising drug targets¹. An important family of proteases are metalloproteases, in particular the metzincins. This family includes matrix metalloproteases (MMPs), disintegrin and metalloproteases (ADAMs), ADAMs with thrombospondin motifs (ADAMTSs), and the astacins. The latter comprises bone-morphogenetic protein 1 (BMP-1), ovastacin, and the meprins α and β in human². However, unlike MMPs or ADAMs, astacins received only a little attention in drug discovery in the past. Nevertheless, continuously growing knowledge of astacin biology increases the evidence that they are potential drug targets as well. In particular, meprin α and β seem to be involved in the pathophysiology of various diseases. Thus, they emerged as promising drug targets during the last years. While meprin α is expressed as soluble homodimer, meprin β homodimers mainly remain membrane-bound, but can also be shed from the cell surface^{3,4}. In tissues co-expressing both meprins, meprin α is also bound to the cell membrane via the formation of meprin α/β heterodimers⁵. These differences in expression and localisation also determine different cleavage specificities and thus different roles in health and disease.^{6,7} Meprin α is supposed to act as pro-migratory protease in the context of colorectal and hepatocytic cancer^{8–13} and was also linked to vascular diseases like arteriosclerosis, cardiac remodelling, and aneurysms,

recently^{14–16}. Meprin β is also involved in cancer cell invasion^{17,18} and moreover is able to act as an alternative beta-secretase, contributing to the progression of Alzheimer's disease via the release of neurotoxic amyloid peptides^{4,19–23}. Both proteases act as procollagenases and are involved in the biosynthesis and assembly of collagen fibrils. Hence, they are potentially involved in the development of fibrotic diseases, e.g. keloids or lung fibrosis^{24–26}. Further substrates include different cytokines and components of the extracellular matrix, rendering meprin α and β potential drug targets in inflammatory or kidney diseases^{27–33}.

The abovementioned roles in pathophysiology suggest meprin α and β as valuable drug targets, but further target validation is needed to shed light on their individual contribution to the onset of diseases and potential treatment options. For this purpose, highly potent and selective inhibitors are required that could serve as lead compounds for preclinical development and/or chemical probes to elucidate the impact of pharmacological modulation of meprin activity on disease progression. However, no inhibitor of either meprin α or β has entered clinical trials, yet. In general, the development of metalloprotease inhibitors, in particular MMP inhibitors, was impaired in the past and the occurrence of undesired side-effects led to the discontinuation of clinical development³⁴. Most metalloprotease inhibitors rely on a hydroxamic acid moiety as zinc chelating group. However, due to the strong hydroxamate-zinc interaction this could cause inhibition of other metalloproteases and also other zinc-dependent enzymes. In consequence, this unselective off-target inhibition can lead to the observed side effects³⁵. Hence, it is of particular importance to monitor the inhibition of related enzymes

CONTACT Daniel Ramsbeck  daniel.ramsbeck@izi.fraunhofer.de  Department of Drug Design and Target Validation MWT, Fraunhofer Institute for Cell Therapy and Immunology IZI, Biocenter, Weinbergweg 22, Halle (Saale), 06120, Germany

*Present address: Mirko Buchholz, PerioTrap Pharmaceuticals GmbH, Halle (Saale), Germany.

 Supplemental data for this article is available online at <https://doi.org/10.1080/14756366.2023.2165648>

© 2023 The Author(s). Published by Informa UK Limited, trading as Taylor & Francis Group.

This is an Open Access article distributed under the terms of the Creative Commons Attribution-NonCommercial License (<http://creativecommons.org/licenses/by-nc/4.0/>), which permits unrestricted non-commercial use, distribution, and reproduction in any medium, provided the original work is properly cited.

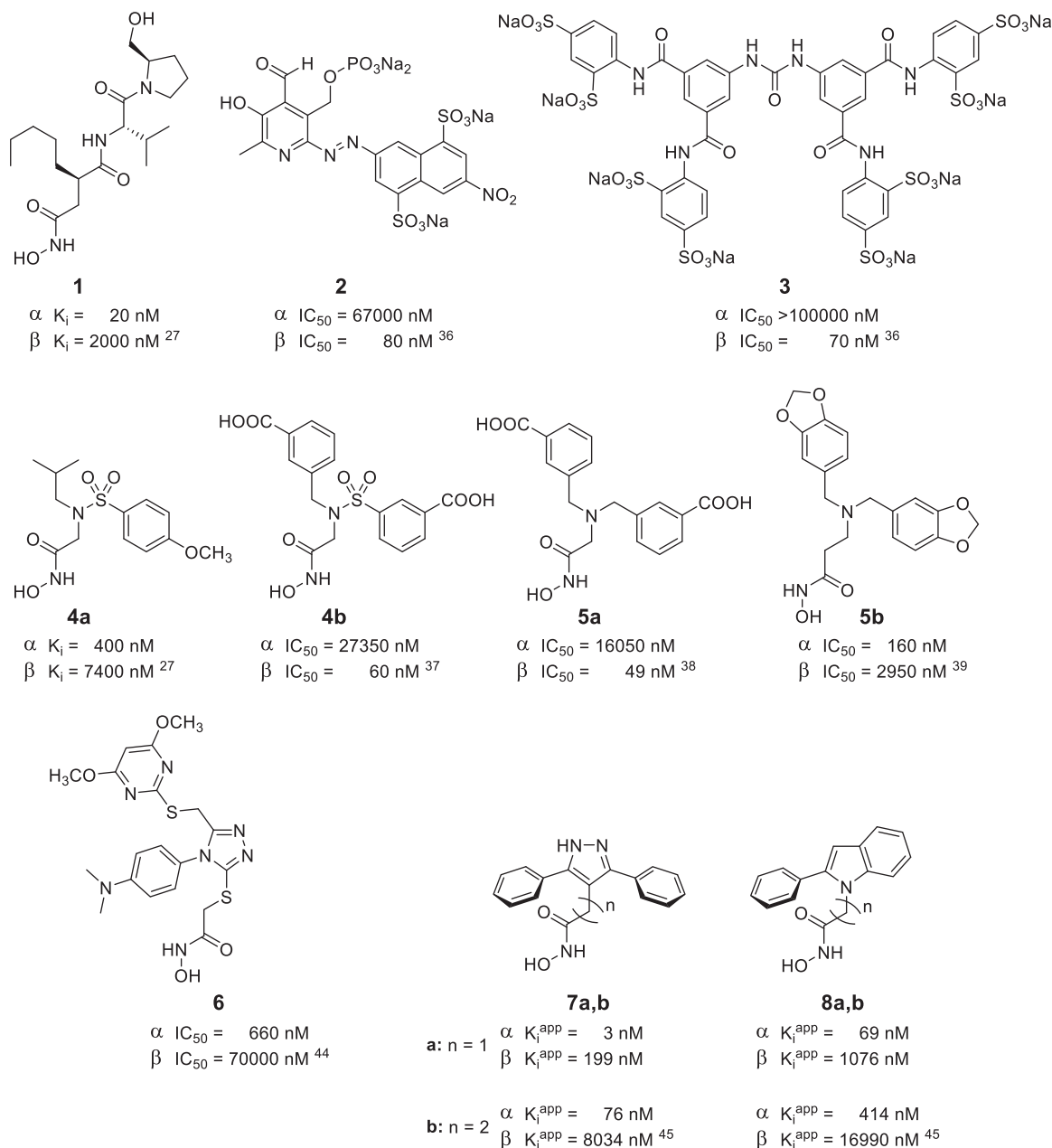


Figure 1. Examples of known inhibitors of meprin α and β .

during the development of metalloprotease inhibitors. Potent inhibitors of both meprin isoenzymes are already known (Figure 1). The first inhibitors of meprins have been reported by Kruse et al., e.g. the naturally occurring Actinonin (**1**) or the broad spectrum metalloprotease inhibitor NNGH (**4a**)²⁷. Later, novel chemotypes have been identified by high throughput screening (**2** and **3**)³⁶. The first systematic elaboration of structure–activity relationship (SAR) using NNGH as lead structure led to the development of potent sulfonamide (**4b**) and tertiary amine based inhibitors (**5a,b**)^{37–39}. The latter exhibit favourable inhibition of either meprin β or α , respectively. Notably, these inhibitors also contain a hydroxamic acid moiety as zinc-chelating functionality, bearing the abovementioned potential risk of unselective off-target inhibition. Nevertheless, they exhibit a superior selectivity profile against off-target metalloproteases, a prerequisite for further development and a potential clinical application. The SAR of the sulfonamide and tertiary amine based inhibitors revealed the importance of an acidic scaffold decoration to achieve potent inhibition of meprin β ^{37,38,40}. This corroborates its substrate

specificity, with a high preference of acidic amino acids in P1 and P1'-position of the respective substrates. This is mediated by a cluster of positively charged arginine residues in the active site cleft, forming the S1, S1', and S2' pocket, respectively⁴¹. Although the S1'-pocket in meprin α comprises an arginine as well, the prevalence for acidic substrates is less pronounced, due to differing amino acids shaping the S1 and S2' pockets, i.e. tyrosine residues^{41,42}. This also translates into the structural requirements for meprin α inhibitors, being less acidic and also neutral moieties could lead to sufficient activity.

More recently, novel heteroaromatic inhibitors of meprins have been reported that were discovered by high throughput screening (**6**) or scaffold-hopping (e.g. **7a,b** and **8a,b**)^{43–45}. The latter monocyclic or fused heteroaromatic derivatives represent the most potent inhibitors of meprins that have been reported to date, even without any functionalization of the actual diaryl-heteroaromatic scaffold. Since they also exhibit a favourable selectivity profile over other metalloproteases, these heteroaromatic derivatives represent promising lead structures. Thus, we aimed at

further optimisation of heteroaromatic inhibitors in the present study. We considered the pyrazole scaffold as particularly suitable for further structural modifications, since the 3,5-diphenylpyrazole (**7a**) already exhibited high potency against meprin α . Moreover, the synthesis of pyrazole derivatives is quite established and thus enables a straightforward SAR exploration. Thus, modifications in positions 3 and 5, covering symmetric and unsymmetrical substitution, were evaluated to modulate the inhibitory activity and selectivity between meprin α and meprin β .

Based on our previous docking studies, the aryl moieties are targeting most likely the S1 and S1'-pocket of meprin α and β . Hence, the introduction of different functional groups was expected to modulate the activity against both meprins by addressing the conserved arginine residue in S1' or modulate the selectivity for either isoenzyme by interacting with the S1 site, formed by tyrosine in meprin α vs. arginine in meprin β . To address additional binding pockets, e.g. the S2' pocket, we also aimed at the introduction of *N*-substituted pyrazoles to further modulate the activity of the inhibitors (Figure 2).

Like the S1 pocket, S2' differs in both meprins as well, i.e. tyrosine in meprin α and arginine in meprin β . Hence, these modifications could also contribute to alter the selectivity profiles against the individual isoenzymes.

Results and discussion

Synthesis

The 3,4,5-substituted pyrazole derivatives were synthesised starting from 3-benzoyl propionic acid derivatives **11a–e**, that were either commercially available or have been synthesised from the respective acetophenones (**9a–d**, Scheme 2). For compounds with variations of only one aryl moiety (**14a–t**, Table 1) commercially available 3-benzoylpropionic acid (**11a**) was used as depicted in Scheme 1. The protected hydroxamic acid was introduced by

coupling with benzylhydroxylamine yielding *N*-benzyloxy-4-oxo-4-phenylbutanamide (**12a**). The formation of the pyrazole core was accomplished using a one-pot method reported by Heller et al.⁴⁶ The 1,3-diketone intermediates were synthesised from **12a** and either acid chlorides for **13a–f** or carboxylic acids and carbonyldiimidazole (CDI) for **13g–p** and **r–t** or the respective anhydride for **13q**. The 1,3-diketones were converted *in situ* into the respective pyrazoles (**13a–t**) by subsequent addition of hydrazine monohydrate.

Derivatives bearing acidic functional groups were introduced using a suitable protecting group, i.e. methyl ester for **13j,k,r,s**, and **t**, methyl ether for **13l** and **m**, benzyl ether for **13n**, *tert*-butyl for **13o** and *para*-methoxybenzyl for **13p**. The cleavage of the hydroxamic acid benzyl protecting group was accomplished by hydrogenation (**14d–g**). Alternatively, boron tribromide enabled the concomitant cleavage of methoxy-protected groups of phenol residues (**14l** and **m**), carboxylic acid esters (**14j,k,r–t**), benzyl ether of the 3-hydroxy-isoxazole residue (**14n**), *tert*-butyl protecting group of the trifluoromethyl pyrazole residue (**14o**), *para*-methoxybenzyl protecting group of tetrazole residue (**14p**) and the benzyl-protecting group of the hydroxamic acid.

The pyrazole derivatives with variations of both aryl moieties (**16a–m**, Table 2) were synthesised starting from the respective acetophenones **9a–d** as depicted in Scheme 2. After alkylation with either methyl bromoacetate (**10a**) or *tert*-butyl bromoacetate (**10b–d**), the protecting group of the 3-benzoylpropionic acid ester derivatives (**10a–d**) was cleaved by either basic or acidic conditions to yield the corresponding 3-benzoylpropionic acids (**11b–e**). The protected hydroxamic acid was introduced by coupling **11b–e** with benzylhydroxylamine. The formation of the pyrazole core was again accomplished as described above by the method reported by Heller et al.⁴⁶ using either acid chlorides or carboxylic acids and carbonyldiimidazole (CDI), followed by subsequent addition of hydrazine monohydrate, yielding the protected pyrazole derivatives **15a–m**.

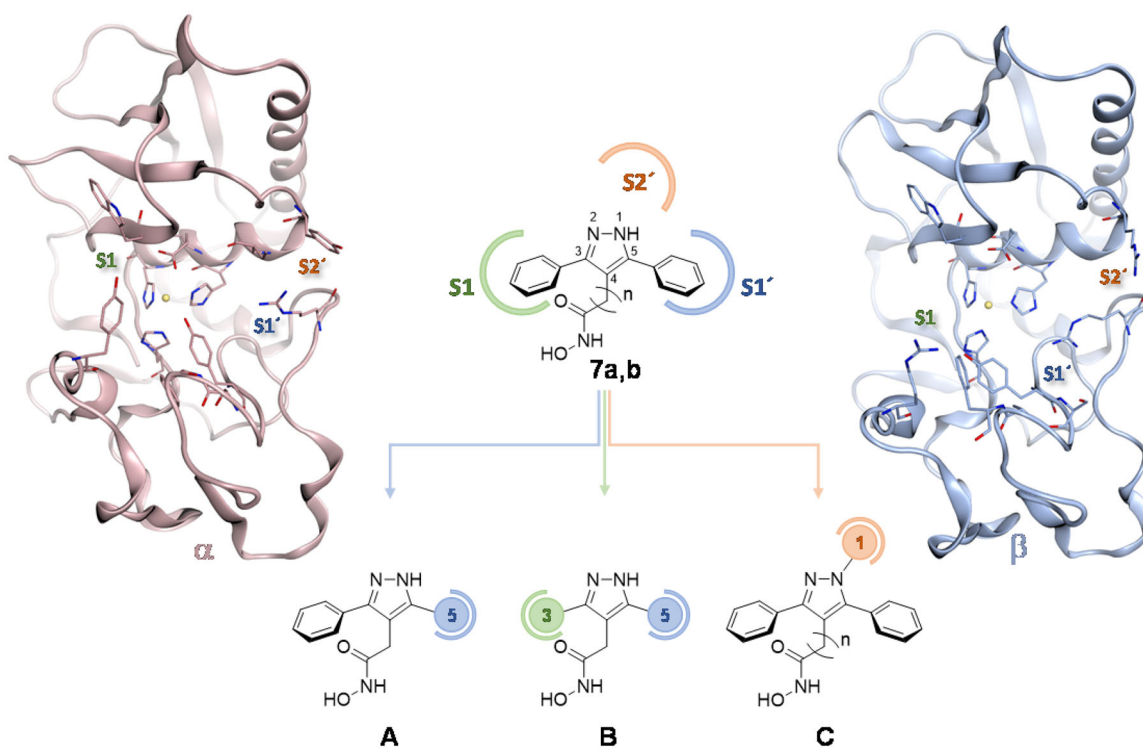
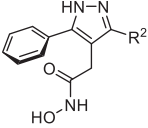
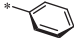
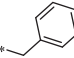
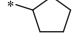
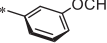
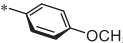
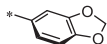
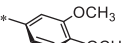
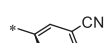
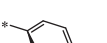
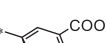

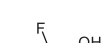

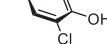
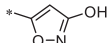
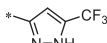
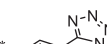





Figure 2. Protease domains of meprin α and β . Possible modifications of the pyrazole scaffold to address and modulate interactions with the S1, S1', or S2' pocket of meprin α and β are depicted.

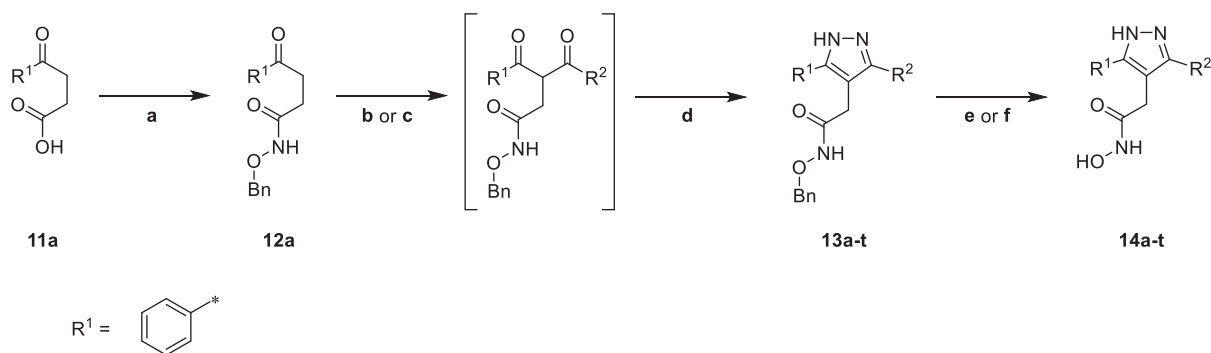
Table 1. Inhibition of meprin α and β by 3,4,5-substituted pyrazoles (structural variation of one aryl moiety).

		$K_i^{(app)}$ (nM) ^a		
		Meprin α	Meprin β	SF
7a		1.3 (1.19)	115.8 (1.08)	116
14a	*-CH ₃	302.0 (1.12)	2110.8 (1.10)	7
14b		69.7 (1.05)	1733.4 (1.11)	25
14c		5.6 (1.11)	319.7 (1.06)	53
14d		1.1 (1.10)	116.0 (1.14)	105
14e		1.3 (1.14)	62.0 (1.04)	48
14f		1.1 (1.09)	109.1 (1.09)	99
14g		0.7 (1.31)	83.2 (1.05)	117
14h		4.8 (1.10)	334.7 (1.06)	67
14i		13.6 (1.04)	995.0 (1.14)	71
14j		7.5 (1.33)	47.5 (1.16)	6
14k		17.2 (1.16)	116.0 (1.15)	7
14l		2.2 (1.23)	60.6 (1.10)	31
14m		0.1 (1.62)	0.4 (1.14)	3
14n		15.9 (1.26)	13.9 (1.08)	1
14o		1.6 (1.14)	88.4 (1.12)	55
14p		0.7 (1.09)	6.7 (1.15)	10
14q		0.3 (1.35)	32.6 (1.16)	127
14r		1.4 (1.25)	54.5 (1.15)	39
14s		11.6 (1.15)	97.7 (1.09)	8
14t		9.9 (1.18)	34.9 (1.15)	4

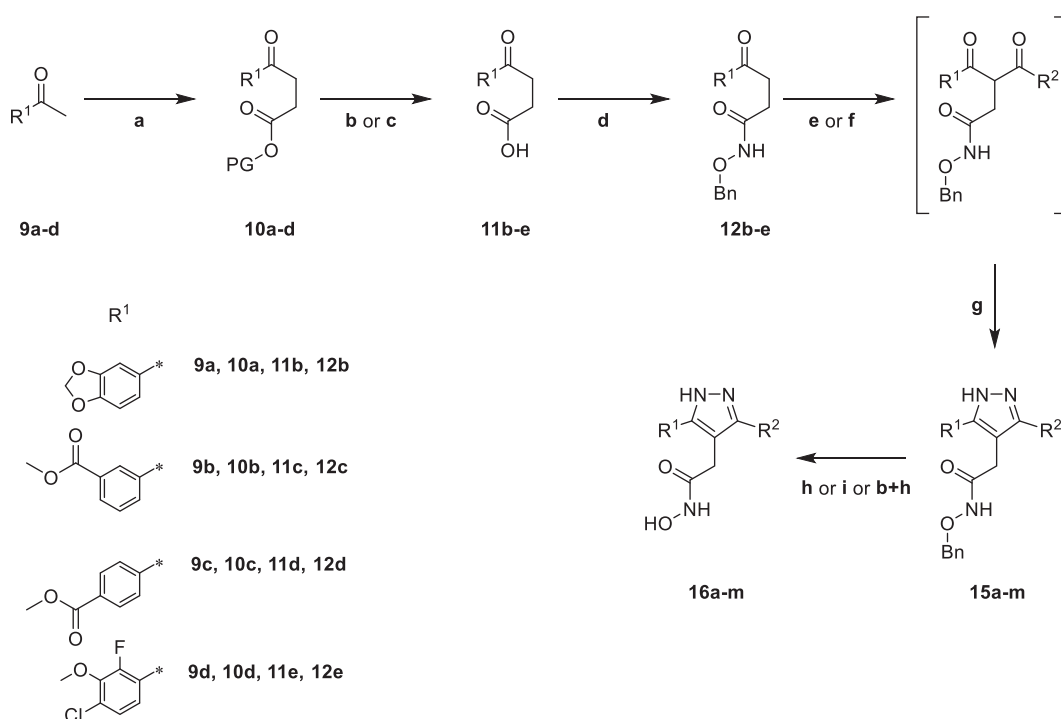
SF: selectivity factor ($K_i^{(app)}$ meprin β / $K_i^{(app)}$ meprin α).^aGeometric mean of three independent experiments with standard deviation factor.

Depending on the protecting groups, the final deprotection was carried out in different manners. The cleavage of the benzyl protecting group was accomplished by hydrogenation (**16a**). Alternatively, boron tribromide enabled the concomitant cleavage of methoxy-protected groups of phenol residues, carboxylic acid

esters, and the benzyl-protecting group of the hydroxamic acid (**16b-d, g-j, l, m**). Derivatives bearing an ester residue could not be treated with boron tribromide if another unstable or susceptible group was present, i.e. a benzodioxolane (**16e,f**) or 1,2-cyclohexanecarboxylic acid (**16k**), and were deprotected via basic



Scheme 1. Synthesis of 3,5-diarylpyrazole hydroxamic acid derivatives with variation of one aryl moiety. Reagents and conditions: (a) Bn-OH₂*HCl, TBTU, DIPEA, DMF, RT (66%); (b) R²-COCl or acid anhydride, LiHMDS, toluene, 0 °C to RT (for **13a-f,q**, 26–74%); (c) i: R²-COOH, CDI, THF, RT, ii: LiHMDS, toluene, 0 °C to RT (for **13g-p,r-t**, 16–90%); (d) N₂H₄*H₂O, AcOH, toluene, EtOH, THF, RT to 50 °C; (e) H₂, 4 bar, Pd/C, MeOH/THF (1:1, v/v), RT (for **14d-g**, 41–82%); (f) BBr₃, DCM, 0 °C to RT (for **14a-c** and **h-t**, 2–45%).



Scheme 2. Synthesis of functionalised 3,5-diarylpyrazole hydroxamic acid derivatives with variation of both aryl moieties. Reagents and conditions: (a) BrCH₂COOME for **10a**, BrCH₂COOtBu for **10b-d**, DMPU, LiHMDS, THF, –60 °C to RT (60–100%); (b) LiOH*H₂O, THF/H₂O (3:1, v/v), RT (for **11b**, 99%); (c) TFA/DCM (1:1, v/v), RT (for **11c-e**, 71–99%); (d) Bn-OH₂*HCl, TBTU, DIPEA, DMF, RT (48–78%); (e) R²-COCl or acid anhydride, LiHMDS, toluene, 0 °C to RT (for **15a,k**); (f) i: R²-COOH, CDI, THF, RT, ii: LiHMDS, toluene, 0 °C to RT (for **15b-j,l,m**); (g) N₂H₄*H₂O, AcOH, toluene, EtOH, THF, RT to 50 °C (7–56%); (h) H₂, 4 bar, Pd/C, MeOH/THF (1:1, v/v, for **16a,e,f,k**, 10–69%), RT; (i) BBr₃, DCM, 0 °C to RT (for **16b-d, g-j, l, m**, 1–26%).

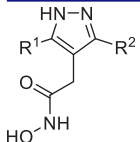
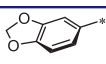
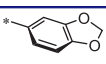
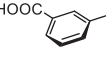
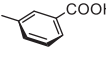
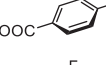
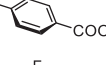
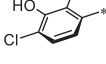
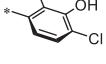
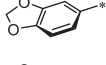
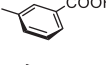
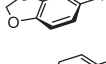
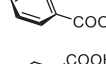
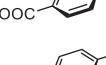
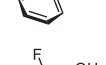
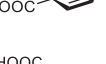
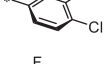
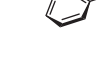
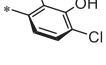
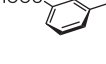
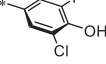
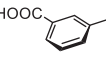

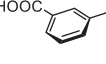
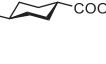
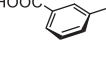

hydrolysis to the corresponding carboxylic acid and hydrogenation for benzyl deprotection.

The synthesis of *N*-substituted 3,5-diphenylpyrazoles (**21a-i** and **22**, Table 3) was accomplished starting from 3,5-diphenylpyrazole ester derivatives (**17** and **18**) as depicted in Scheme 3. The 3,5-diphenylpyrazole methyl esters as starting materials could be obtained by cyclocondensation of the respective 1,3-diphenylpropan-1,3-diones and hydrazine dihydrochloride (Supporting Information).

The introduction of diverse substituents was carried out by different approaches. Alkyl or benzyl moieties were introduced by *N*-alkylation using sodium hydride and the respective alkyl or benzyl halides at room temperature (**21a, e-i**, **22**). The *N*-substituted pyrazole ester intermediates (**19** and **20**) were converted to the respective hydroxamates by means of hydroxylamine

hydrochloride under microwave irradiation. Compounds with carboxylic acid groups as part of substituent R³ (**21g** and **h**) were introduced using *tert*-butyl protected building blocks and were deprotected under acidic conditions using trifluoroacetic acid in dichloromethane before the conversion of the methyl ester to the hydroxamic acid was accomplished by means of hydroxylamine hydrochloride under microwave irradiation, as described above. Pyrazole derivatives bearing a phenol residue within group R³ (**21i** and **22**) required an additional deprotection step using boron tribromide to cleave the methoxy protecting group after the conversion of the methyl ester to the respective hydroxamic acid. The introduction of *N*-aryl moieties (**21b-d**) was accomplished by Chan-Lam coupling using the corresponding phenyl boronic acid and the trityl-protected pyrazole hydroxamate with C₁ spacer (**23**). The trityl-protected analogues (**24a-c**) were treated with

Table 2. Inhibition of meprin α and β by 3,4,5-substituted pyrazoles (structural variation of both aryl moieties).

			$K_i^{(app)}$ (nM) ^a		
			Meprin α	Meprin β	SF
16a			0.6 (1.08)	112.9 (1.12)	177
16b			9.9 (1.00)	14.5 (1.22)	1
16c			55.8 (1.03)	116.3 (1.01)	2
16d			4.2 (1.08)	13.9 (1.12)	3
16e			3.1 (1.14)	44.4 (1.04)	15
16f			10.5 (1.05)	92.8 (1.02)	9
16g			20.3 (1.02)	32.5 (1.17)	2
16h			9.6 (1.05)	11.2 (1.06)	1
16i			5.1 (1.02)	4.0 (1.51)	1
16j			0.1 (1.35)	0.2 (1.13)	2
16k			0.4 (1.21)	5.2 (1.16)	13
16l			19.8 (1.10)	20.9 (1.16)	1
16m			21.0 (1.14)	14.5 (1.08)	0.7

SF: selectivity factor ($K_i^{(app)}$ meprin β / $K_i^{(app)}$ meprin α).^aGeometric mean of three independent experiments with standard deviation factor.

trifluoroacetic acid in dichloromethane yielding the respective *N*-aryl pyrazoles (**21b–d**).

Structure–activity relationships

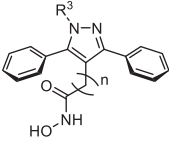
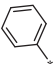
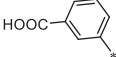
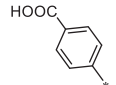
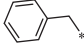
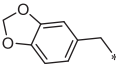
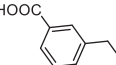
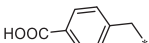
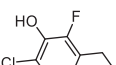
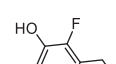
For exploration of the SAR, the structural variation of one moiety at position 3(5) of the 3,4,5-substituted pyrazoles was initially evaluated (Table 1). The 3,5-diphenylpyrazole **7a** without any further functionalization of the phenyl moieties already exhibited a high inhibitory activity against meprin α in the low nanomolar range. The introduction of residues with different sizes, i.e. methyl (**14a**) or benzyl group (**14b**) revealed a decrease in inhibitory activity, whereas the pyrazole derivative bearing a cyclopentyl moiety (**14c**) exhibited similar activities compared to **7a**. This underpins the predicted binding mode of the heteroaromatic inhibitors from previous docking studies, that suggested one phenyl substituent being orientated towards the S1'-subsite⁴⁵. Thus, the lack of interactions of the methyl moiety or a different orientation by the benzyl moiety within the S1'-binding site could lead to a decrease in meprin inhibition. The introduction of a cyclic moiety, directly

connected to the pyrazole core is favourable for the inhibition of meprin α and β and might address the S1'-subsite like the phenyl residue found in **7a**. Since the phenyl moiety was determined to be most favoured, a series of structural modifications of the phenyl moiety was further explored and revealed inhibitory activities in the nanomolar and even picomolar range (Table 1, **14d–p**).

Electron rich moieties (**14d–14g**) were tolerated for the inhibition of meprin α and β , but electron deficient cyanoaryl moieties (**14h**, **14i**) led to reduced activity against meprin α and β . However, the introduction of different electron rich moieties, such as methoxyphenyl groups (**14d**, **14e**) did not lead to a further increase in inhibitory activity compared to the unsubstituted 3,5-diphenylpyrazole **7a** and also the increase of the electron density with the introduction of a benzodioxolane (**14f**) or dimethoxyphenyl moiety (**14g**) had no major impact on the binding affinities.

For pyrazole derivatives bearing acidic carboxyphenyl moieties (**14j**, **14k**), an increased activity against meprin β in the case of a *meta*-substitution could be observed. Nevertheless, the compounds still remained more active against meprin α , although the potency was slightly reduced compared to **7a**. To elaborate the

Table 3. Inhibition of meprin α and β by *N*-substituted 3,5-diphenylpyrazoles.

		R^3	n	$K_i^{(app)}$ (nM) ^a		SF
				Meprin α	Meprin β	
7a		H _*	1	1 (1.19)	116 (1.08)	116
21a		H ₃ C _*	1	5 (1.02)	437 (1.08)	87
21b			1	4 (1.04)	667 (1.09)	167
21c			1	4 (1.08)	212 (1.06)	53
21d			1	4 (1.12)	182 (1.09)	46
21e			1	1 (1.08)	291 (1.12)	291
21f			1	0.6 (1.23)	305.0 (1.02)	508
21g			1	0.3 (1.12)	10.6 (1.14)	35
21h			1	0.4 (1.36)	9.4 (1.16)	24
21i			1	0.08 (1.30)	9.3 (1.04)	116
22			2	0.15 (1.26)	1183.8 (1.09)	7892

SF: selectivity factor ($K_i^{(app)}$ meprin β / $K_i^{(app)}$ meprin α).

^aGeometric mean of three independent experiments with standard deviation factor.

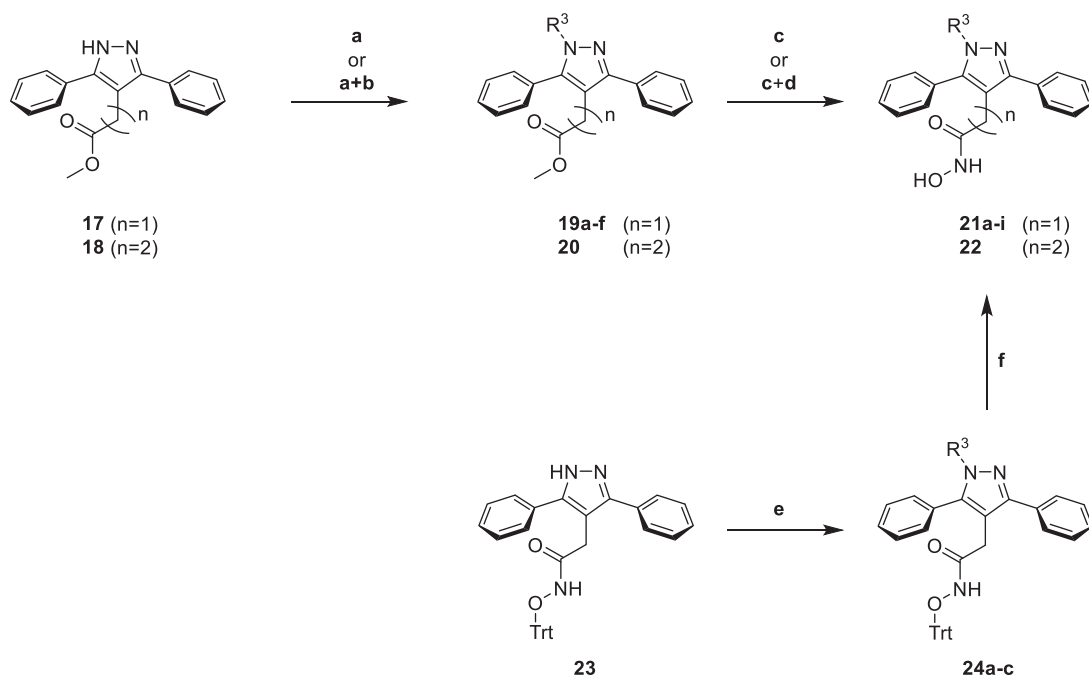
influence of acidic substituents further, the introduction of carboxylic acid bioisosters (**14l–14p**) was evaluated, resulting in a general improvement of activity against meprin β . A minor increase in the potency against meprin β could be observed for pyrazoles bearing a halogenphenol in *meta*-position (**14l**) and trifluoromethyl pyrazole moiety (**14o**). A further improvement in activity against meprin β by factor 16 compared to **7a** could be achieved with the introduction of a phenyltetrazole moiety (**14p**), although this compound is still a more potent inhibitor of meprin α .

An equipotent inhibition of both meprin isoenzymes could be observed with the halophenol (**14m**) and 3-hydroxy-isoxazol moiety (**14n**). The introduction of the acidic phenol in *para*-position (**14m**) led to the strongest increase in activity against meprin α and β , respectively. Hence, this is the most potent small molecule inhibitor of both meprins so far. The high potency of **14m** against meprin α and β , might be visualised by a respective docking pose, which revealed the interaction of the halophenol moiety within the S1'-subpocket (Figure 3). Thus, a possible interaction of the acidic moiety with the corresponding arginine residue (R²⁴² in meprin α , R²³⁸ in meprin β) via ionic interactions or charged hydrogen bonds could contribute to the potent inhibition. Moreover, π - π interactions of the pyrazole core with either Y¹⁸⁷ in meprin α , shaping the S1-subsite, or Y²¹¹ in meprin β are

suggested. For meprin β , the formation of another hydrogen bond involving the phenol and S²¹² could be possible. Such a hydrogen bond network was already observed for the interaction of meprin β with compound **5a**, earlier⁴⁰.

Since the replacement of one phenyl moiety by an aliphatic ring was tolerated (**14c**), also cyclohexylcarboxylic acids were introduced to increase the sp³-content of the compounds (**14q–t**). Regardless of the substitution pattern, an increased potency against meprin β could be observed, comparable to **14j**, suggesting an interaction with arginine in either S1 or S1' pocket of meprin β . However, the activity against meprin α was less affected. In summary, the introduction of acidic substituents generally increases the inhibitory activity against meprin β . This corroborates the preference of meprin β for acidic substrates and also the SAR of the meprin β selective inhibitors reported earlier³⁸. However, since the activity against meprin α was only slightly affected by the respective modifications, a switch towards meprin β selective inhibitors could not be achieved.

Further modification of both phenyl moieties at position 3 and 5 of the pyrazole core (Table 2, **16a–j**) indicated that the introduction of a second substituent had only a marginal impact on the inhibitory activities against meprin α and β in comparison to corresponding monosubstituted pyrazoles bearing the same



Scheme 3. Synthesis of *N*-substituted 3,5-diarylpyrazole hydroxamic acid derivatives. Reagents and conditions: (a) i: NaH, DMF, 0 °C, ii: R³-Hal, 0 °C to RT (**19a–c,f** and **20**, 71–98%); (b) TFA/DCM (1:1, v/v), RT (for **19d,e**, 94–99%); (c) NH₂OH⁺HCl, NaOCH₃, MeOH, microwave, 80 °C (for **21a,e–h**, 5–53%); (d) BBr₃, DCM, 0 °C to RT (for **21i** and **22**, 23–54%); (e) R³-B(OH)₂, Cu(OAc)₂, TEA, molecular sieves 3 Å, DCM, RT (25–30%); (f) TFA/DCM (1:1, v/v), TIS, RT (for **21b–d**, 39–55%).

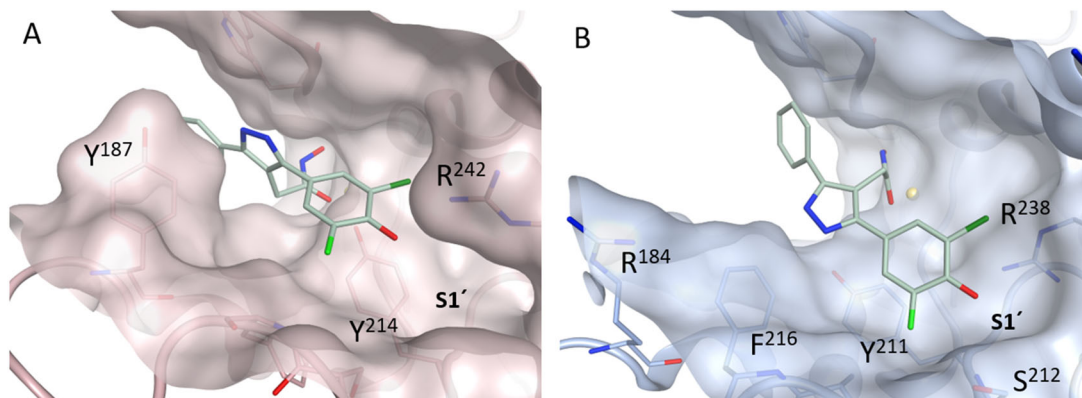


Figure 3. Putative binding mode of **14m** found by docking to the active site of meprin α (A) and meprin β (B).

decoration on R². Nevertheless, the compounds exhibit a further improved selectivity against off-target proteases (vide infra). The introduction of two electron rich moieties (**16a**) led to an inhibitor with similar activities compared to its monosubstituted pyrazole analogue (**14f**). With the combination of an electron rich benzodioxolane moiety with an acidic carboxyphenyl moiety, i.e. compound **16e** and **16f**, a reduction of the meprin α selectivity by factor ~ 10 – 20 could be observed compared to the pyrazole bearing two benzodioxolane moieties (**16a**) underpinning the preference for acidic residues of meprin β for inhibitor binding. To further improve the meprin β activity and selectivity, different combinations of acidic moieties, i.e. carboxyphenyl, cyclohexylcarboxylic acid, and halogenphenol moieties (**16b–d**, **16g–m**) were investigated.

However, the introduction of a second acidic moiety did not lead to a noticeable difference in activity compared to the monosubstituted pyrazole analogues (**14j–m**). The activity against meprin α was not affected or even slightly increased. Hence, albeit the introduction of acidic moieties increases the activity against meprin β , these modifications did not lead to an improvement in

the meprin β selectivity and just revealed equipotent inhibition of meprin α and β . This is in contrast to the structure-activity relationships of the tertiary amines, where meprin β selectivity could clearly be obtained by the introduction of two acidic substituents that could address arginine residues within the S1' as well as S1-subsite of meprin β ³⁸.

The pyrazole core was found by a scaffold hopping approach to rigidify the tertiary amine scaffold³⁸. Although this was successful and led to a series of highly potent heteroaromatic inhibitors of meprins, in particular against meprin α , these compounds obviously lack a certain degree of flexibility or less suitable binding of the scaffold that is required to achieve meprin β selectivity. The latter seems to be mainly driven by addressing arginine residues in S1 and S1' by ionic interactions of the tertiary amine derived inhibitors. Due to the relatively rigid body of the diphenyl pyrazole core, the acidic moieties obviously cannot be placed in the right position to form the required ionic interactions with both arginine residues in S1 and S1', respectively. Despite their high potency, a high selectivity for meprin β as found for the tertiary amines³⁸ or even a slight preference for meprin β could not be

achieved by the investigated compounds, limiting their pharmacological applicability. Hence, for the generation of inhibitors suitable for selectively addressing meprin β , e.g. to target its secretase function in Alzheimer's disease, the diarylpyrazole scaffold elaborated in the present study might not be as suitable as the tertiary amine scaffold, reported earlier. However, compound **14m** is a highly potent inhibitor of both meprins with a favourable off-target selectivity (vide infra) that might be useful for an application in conditions where an inhibition of both meprins might be useful, e.g. kidney diseases or the processing of procollagen in fibrotic disorders.

In addition to the evaluation of the structural modifications at positions 3 and 5 of the pyrazole, the influence of the *N*-substitution on the binding affinity was elaborated (Table 3). The *N*-substitution was performed from 3,5-diphenylpyrazole **7a**. The introduction of different lipophilic moieties, i.e. methyl (**21a**) and phenyl moiety (**21b**), resulted in a 4- to 6-fold decrease in activity against meprin α and β compared to the unsubstituted 3,5-diphenylpyrazole **7a**. However, the extension of the pyrazole with a benzyl moiety (**21e**) demonstrated no significant reduction of the inhibitory activities, although the potency against meprin β is slightly decreased in comparison to **7a**. Further variation of the *N*-phenyl pyrazole by the introduction of acidic carboxyphenyl residues (**21c**, **21d**) led to an increased inhibition of meprin β by factor 3 in comparison to the *N*-phenyl pyrazole **21b**.

This also corroborates the preference of acidic moieties at this position, in particular for meprin β with an additional arginine in S2', i.e. R¹⁴⁶. Since the introduction of a benzyl moiety at position 1 of the pyrazole (**21e**) was well-tolerated, we assumed that this moiety could be explored for further modifications. The introduction of an electron-rich benzodioxolane moiety (**21f**), that additionally could serve as hydrogen bond acceptor, had only a marginal effect on the inhibitory activity against meprin α compared to the *N*-benzylated pyrazole **21e**. In contrast to that, introduction of acidic moieties had a greater impact on the inhibitory activities. The aromatic carboxylic acid substitutions at a benzylic unit (**21g**, **h**) resulted in a 3-fold improved activity against meprin α and had even a particularly favourable effect on the inhibition of meprin β with a 30-fold increase in potency compared to **21e**. However, this also affected the selectivity of meprin α , which shifted from a three-digit to a two-digit range. The replacement with a bioisosteric halophenol moiety (**21i**) led to a comparable improvement of the potency against meprin β in the lower nanomolar range. However, the halophenol moiety of **21i**, with hydroxyl function in *meta*-position, was much more preferred for the inhibition of meprin α compared to **21g** or **h** and exhibited an increased inhibitory activity in the picomolar range, thus shifting the selectivity of **21i** again more towards a preferred inhibition of meprin α . Our recent study has shown that the extension of the spacer length of the hydroxamic moieties to the

heteroaromatic core led to a reduction of the inhibitory activity against meprin α and β , but slightly increased the selectivity for meprin α ⁴⁵. Similarly, for compound **22** the extension of the spacer length from C1 to C2 spacer again had an impact on the activity and in particular the selectivity of the inhibitor. However, while the activity against meprin α was virtually not affected, the activity against meprin β dropped by factor ~ 120 compared to **21i**, resulting in a $K_i^{(app)}$ value against meprin β in the micromolar range, thus leading to an exceptional high selectivity for meprin α over meprin β with a factor of almost 7900. The combination of this high selectivity and activity outperforms the other inhibitors elaborated in this study, making **22** particularly useful for a pharmacological modulation of meprin α activity and the utilisation as chemical probe for target validation. To obtain a better understanding of the consistently high potency of compound **22** against meprin α , despite the variation of the spacer length, docking studies of **21i** with C1 spacer and **22** with C2 spacer were performed (Figure 4).

The resulting docking solutions revealed binding poses of the *N*-substituted diphenylpyrazole **21i** and **22** that differ from the predicted binding mode of the docked 3,4,5-substituted pyrazole **14m** in meprin α . While the docking solution of **14m** involves π - π interactions of the pyrazole core with Y¹⁸⁷ in the S1-subpocket, the *N*-substituted pyrazole **21i** and **22** are moved away from the S1-subsite. Regardless of the spacer length, the halophenol moiety of both, **21i** and **22**, could address the S1'-subsite via an ionic interaction or charged hydrogen bond to arginine residue R²⁴². Moreover, this predicted shift of the binding mode enables one phenyl moiety to interact with an additional lipophilic subpocket, shaped by I¹⁵², A¹⁵¹, and L²¹¹, thus further increasing the binding affinity via hydrophobic contacts. Based on the docking solutions, this interaction might be more favoured in the case of **22**, since the longer spacer allows the ligand to plunge deeper in this pocket. The positioning of the pyrazole derivative **21i** with C1 spacer could also enable π - π interactions of Y¹⁸⁷ and the phenyl moiety. The extension of the spacer length leads to a slightly different positioning of the diphenylpyrazole **22** with C2 spacer within the active site compared to the shorter analogue **21i**, thus ruling out potential π - π interactions with Y¹⁸⁷. According to the predicted binding mode, both inhibitors are able to form an additional Cl- π interaction⁴⁷. This interaction involving the halophenol moiety and Y¹⁴⁹ in S2' of meprin α would contribute to the activity against meprin α and also to the selectivity against meprin β . In meprin β , S2' is formed by an arginine residue, thus ruling out the respective interaction with the halogen of the inhibitor. Additionally, the extension of the spacer from C1 to C2 enhances the selectivity, most likely due to steric reasons. However, the exceptional high selectivity of **22**, i.e. factor 7900, cannot be deduced from the obtained docking results.

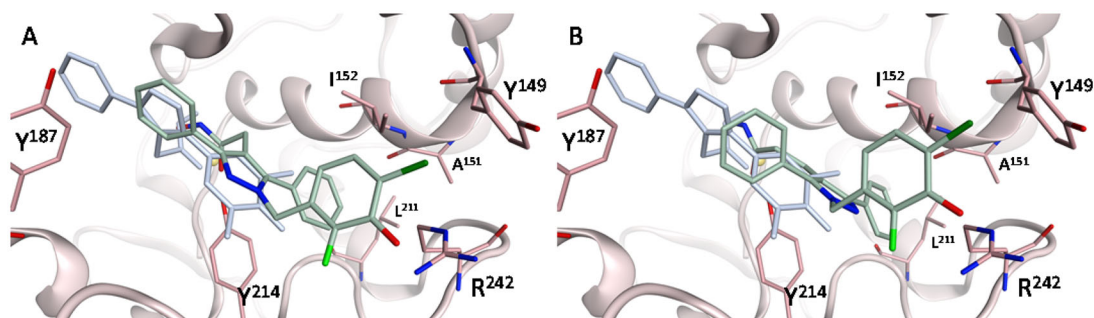


Figure 4. Docking solutions of **21i** (A) and **22** (B) to the active site of meprin α in comparison to **14m** (light blue).

Selectivity profile and *in vitro* toxicity

The evaluation of the heteroaromatic inhibitors already revealed a favourable selectivity profile over the inhibition of selected off-target metalloproteases⁴⁵. With the structural variation of the 3,5-diphenylpyrazole (**7a**) further studies of selected derivatives for possible alterations in off-target selectivity were performed (Table 4). The introduction of several substituents at position 3(5) (**14d**, **14f**, **14g**, **14m**) led to minor alterations in the inhibition of matrix metalloproteases (MMPs) and A Disintegrin And Metalloproteinases (ADAMs) compared to **7a**. The off-target selectivity was more affected by the structural modification of the second aryl moiety, as a pyrazole bearing two benzodioxolane moieties (**16a**) exhibited a higher inhibition of the related metalloproteases, particularly MMP2 with a residual activity of 29% at 10 μ M inhibitor concentration. By contrast, the introduction of two acidic moieties (**16j**) abolished the inhibition of the respective MMPs and ADAMs that led to an excellent high selectivity with residual activities above 90%. While the modification of both aryl residues at position 3 and 5 did not lead to any differences in the inhibitory activity against meprin α and β , an impact on the inhibition of the off-target metalloproteases could be observed, leading to decreased inhibition even at higher concentrations (not shown). The evaluation of selected *N*-substituted pyrazoles (**21f–i**, **22**) revealed residual activities that are mostly comparable to **7a**, with inhibition <50% at a concentration of 10 μ M, except for a stronger inhibition of MMP2 by **21f**. However, the slightly increased inhibition of individual off-target proteases by a few pyrazole derivatives, i.e. **14d,f** and **16a**, **21f**, corresponds to IC_{50} -values in the micromolar range (Table 5). Thus, with $K_i^{(app)}$ values against meprin α in the low nanomolar and upper picomolar range, the compounds still exhibit high selectivity of at least three orders of magnitude against MMPs and ADAMs. In addition, the cell viability

Table 4. Inhibition of off-target metalloproteases by selected 3,4,5-substituted pyrazole inhibitors.

	Residual activity (%) ^a					Cell viability (%) ^b	
	MMP2	MMP9	MMP13	ADAM10	ADAM17	Hep-G2	SY5Y
7a	104	81	75	73	61	100	92
14d	78	80	85	68	52	104	84
14f	41	72	71	59	51	96	90
14g	83	90	101	87	65	99	85
14m	66	86	88	104	68	103	86
16a	29	63	56	62	57	n.d.	n.d.
16j	95	94	105	90	99	98	110
21f	77	74	78	69	21	103	88
21g	89	83	83	92	84	99	85
21h	85	80	86	91	67	103	88
21i	69	70	84	85	72	107	79
22	102	100	98	117	90	100	98

n.d.: not determined.

^aResidual activity (%) @ 10 μ M inhibitor concentration; mean of at least two independent experiments.

^bInhibitor concentration 30 μ M.

Table 5. Inhibitory activities (IC_{50}) against MMP2, MMP13, ADAM10, ADAM17 of selected compounds.

IC_{50} (μ M) ^a	MMP2	MMP13	ADAM10	ADAM17
14d	n.d.	n.d.	n.d.	11.6 (1.05)
14f	5.3 (1.11)	n.d.	13.9 ^b	7.4 (1.10)
16a	1.4 (1.34)	15.7 (1.53)	12.0 (1.02)	9.6 (1.06)
21f	n.d.	n.d.	n.d.	2.3 (1.22)

n.d.: not determined.

^a IC_{50} (μ M) as geometric mean of two independent experiments with standard deviation factor.

^bOnly single measurement.

of liver and neuronal cell lines was determined for selected compounds, proving no *in vitro* toxicity of the tested compounds.

As mentioned above, selectivity issues and inhibition of off-target proteases have impaired the development of metalloproteases in the past. One reason was attributed to the hydroxamate moiety, that might be able to cause such side effects by inhibition of other metalloenzymes due to the high affinity to metal ions, e.g. zinc.

However, the inhibitors reported herein do not exhibit relevant activity against the screened proteases that are structurally related to meprins. Thus, an application for further studies, i.e. target validation or further preclinical development, is not impaired by this issue. Nevertheless, further profiling should include also metalloproteins beyond the metzincin family of proteases. However, the data is another example, that just the presence of a hydroxamic acid moiety is not necessarily the main reason for unselectivity issues and the combination of this metal chelating group with a suitable scaffold could lead to inhibitors with favourable selectivity profiles.

Conclusion

Based on the emerging roles of meprin α and β in the pathophysiology of various diseases, the inhibition of these astacin proteases could provide novel therapeutic opportunities. Highly potent and selective inhibitors are needed to further assess the therapeutic relevance of the potential targets in target validation experiments. Recently, the discovery of novel heteroaromatic scaffolds for the development of astacin protease inhibitors resulted in a significantly improved inhibitory activity, in particular with respect to the inhibition of meprin α . Demonstrating a favourable off-target selectivity and no *in vitro* cytotoxicity, the heteroaromatic cores were identified as potential lead structures. Therefore, further modifications of the pyrazole scaffold were evaluated. Within this study different structural modifications at positions 1, 3, and 5 of the pyrazole core were explored, yielding novel meprin inhibitors that exhibit high inhibitory activities down to the picomolar range. Structural variations of the substituents enabled the modulation of the selectivity within the meprin isoforms. However, a high selectivity for meprin β , as observed for tertiary amine based inhibitors earlier, could not be achieved for the pyrazole based compounds elaborated in this study. Nevertheless, potent pan-meprin inhibitors and highly potent and selective meprin α inhibitors were discovered. In particular, the remarkable off-target selectivity against related metalloproteases and lacking *in vitro* toxicity of the novel pyrazole derivatives allows the application of these compounds as chemical probes for target validation to further assess the functional roles of meprin proteases, in particular meprin α in the disease progression.

Experimental section

Chemistry

General

Starting materials and solvents were purchased from Aldrich, Activate Scientific, Alfa Aesar, Iris Biotech, and Merck Millipore. The purity of the compounds was assessed by HPLC and confirmed to be $\geq 95\%$. The analytical HPLC-system consisted of a Merck–Hitachi device (model LaChrom) utilising a Phenomenex Luna 5 μ M C18(2) column (125 \times 4.0 mm) with $\lambda = 214$ nm as the reporting wavelength. The compounds were analysed using a gradient at a flow rate of 1 ml/min, whereby eluent (A) was

acetonitrile, eluent (B) was water, both containing 0.04% (v/v) trifluoroacetic acid applying the following gradient: 0 min – 15 min: 5–60% (A), 15 min – 20 min: 60–95% (A), 20–30 min: 95% (A), 30–31 min: 95–5% (A), 31–35 min: 5% (A). The purities of all reported compounds were determined by the percentage of the peak area at 214 nm. ESI-Mass spectra were obtained with an Expression CMS single quadrupole spectrometer (Advion). The high-resolution positive ion ESI mass spectra were obtained from a LTQ Orbitrap XL (Thermo Fisher Scientific). The ^1H NMR spectra were recorded at a Bruker Avance III 400 or 700 MHz. DMSO- d_6 was used as solvent unless otherwise specified. Chemical shifts are expressed as parts per million (ppm). The solvent was used as internal standard. Splitting patterns have been designated as follows: s (singlet), d (doublet), dd (doublet of doublet), t (triplet), m (multiplet), and br s (broad signal). The reported target compounds occur as an equilibrium mixture of *E/Z* conformational isomers with regard to the hydroxamic acid moiety^{48,49}. Hence, proton shifts are listed with the respective comment: mixture of *E/Z* isomers. Semi-preparative HPLC was performed on a Prepstar device (Varian) equipped with a Phenomenex Luna 10 μM C18(2) column (250 \times 21 mm). The compounds were eluted using the same solvent system as described above, applying a flow rate of 21 ml/min.

General method for the synthesis of 3-benzoylpropionic acid ester derivatives 10a–d

The respective acetophenone derivative (1 equiv) was dissolved in dry toluene ($c = 1\text{ M}$). After the solution was cooled to -60°C , *N,N'*-dimethylpropyleneurea (DMPU, 3.6 equiv), and lithium bis(trimethylsilyl)amide (LiHMDS, 1 M in THF, 1.2 equiv) were added via syringe under argon atmosphere. After 30 min of stirring, methyl bromoacetate or *tert*-butyl bromoacetate (1.5 equiv) was added dropwise. The mixture was stirred for an additional 10 min, then allowed to warm up to room temperature and stirred for further 5 h. The volatiles were evaporated and the remains were taken up with a small amount of water. The aqueous layer was slightly acidified by means of diluted aqueous HCl (1 M) and was extracted with EtOAc (3 \times 25 ml). The combined organic layers were dried over Na_2SO_4 and evaporated. The residue was purified by flash chromatography (silica, heptane/diethyl ether, or heptane/EtOAc gradient).

General method for the synthesis of 3-benzoylpropionic acids 11b–e

Method A: The respective methyl ester derivative was dissolved in THF/water (3:1 v/v, $c = 0.4\text{ M}$). LiOH $\cdot\text{H}_2\text{O}$ (2 equiv) was added and the mixture was stirred overnight at room temperature. The volatiles were evaporated and the remains were taken up in water, acidified by means of diluted aqueous HCl (1 M), and extracted with EtOAc (3 \times 25 ml). The combined organic layers were dried over Na_2SO_4 and evaporated. The residue was used without further purification.

Method B: The respective *tert*-butylester derivative was treated with TFA/DCM (1:1 v/v, 10 ml) at 0°C and stirred for 2–4 h. The volatiles were evaporated, and the remains were purified by flash chromatography (silica, heptane/EtOAc gradient).

General method for the synthesis of *O*-benzyl hydroxamic acid derivatives 12a–e

The respective 3-benzoylpropionic acid (1 equiv) was dissolved in DMF ($c = 0.5\text{ M}$). 2-(1H-benzotriazole-1-yl)-1,1,3,3-tetramethylammonium tetrafluoroborate (TBTU, 1 equiv) and *N,N*-

diisopropylethylamine (DIPEA, 1 equiv) were added to the solution and the mixture was stirred at room temperature for several minutes. Subsequently *O*-benzylhydroxylamine hydrochloride (1 equiv) and DIPEA (3.2–4 equiv) were added and the mixture was stirred at room temperature for another 3 h. The reaction was quenched with water and extracted with EtOAc (3 \times 25 ml). The combined organic layers were dried over Na_2SO_4 and evaporated. The residue was purified by flash chromatography (silica, heptane/EtOAc gradient).

General method for the synthesis of 3,4,5-substituted pyrazole derivatives 13a–t, 15a–m

Method A: The respective *N*-benzyloxy-4-oxo-4-phenylbutanamide derivative (1 equiv) was dissolved in dry toluene ($c = 0.4\text{ M}$) in a flask sealed with a septum. The solution was cooled to 0°C under argon. LiHMDS (1 M in THF, 2.1 equiv) was added quickly via syringe and the mixture was stirred for 5 min. The respective acyl chloride derivative (0.5 equiv) was added in one portion and the mixture was allowed to warm up to room temperature. The mixture was stirred vigorously until thin-layer chromatography (TLC) showed full conversion of the acyl chloride. AcOH (2 ml) was added to the mixture. EtOH (10 ml) and THF (5 mL) were added to form a homogeneous mixture, then $\text{N}_2\text{H}_4\cdot\text{H}_2\text{O}$ (34.3 equiv) was added. The mixture was heated to 50°C and the reaction was monitored via TLC. The volatiles were evaporated and the remains were taken up in water, acidified by means of diluted aqueous HCl (1 M), and extracted with EtOAc (3 \times 25 ml). The combined organic layers were dried over Na_2SO_4 and evaporated. The residue was purified by flash chromatography (silica, $\text{CHCl}_3/\text{MeOH}$ gradient).

Method B: The respective carboxylic acid derivative (0.5 equiv) was dissolved in dry THF ($c = 0.3\text{ M}$). Under argon atmosphere CDI was added to the solution. The mixture was stirred for 1 h at room temperature. In a separate flask, the respective *N*-benzyloxy-4-oxo-4-phenylbutanamide derivative (1 equiv) was dissolved in dry toluene ($c = 0.4\text{ M}$) and sealed with a septum. The solution was cooled to 0°C under argon. LiHMDS (1 M in THF, 2.1 equiv) was added quickly via syringe and the mixture was stirred for 5 min. The respective activated carboxylic acid derivative (0.5 equiv) was added in one portion and the mixture was allowed to warm up to room temperature. The mixture was stirred vigorously until TLC showed full conversion of the carboxylic acid derivative. AcOH (2 ml) was added to the mixture. EtOH (10 ml) and THF (5 mL) were added to form a homogeneous mixture, then $\text{N}_2\text{H}_4\cdot\text{H}_2\text{O}$ (34.3 equiv) was added. The mixture was heated to 50°C and the reaction was monitored via TLC. The volatiles were evaporated and the remains were taken up in water, acidified by means of diluted aqueous HCl (1 M), and extracted with EtOAc (3 \times 25 ml). The combined organic layers were dried over Na_2SO_4 and evaporated. The residue was purified by flash chromatography (silica, $\text{CHCl}_3/\text{MeOH}$ gradient).

General methods for deprotection of hydroxamic acid derivatives 14a–t, 16a–m

Method A: The respective benzyl-protected hydroxamic acid was dissolved in DCM (5 ml) in a sealed flask under argon atmosphere. The mixture was cooled down to 0°C and treated with BBr_3 (1 M in DCM, 3–19 equiv). The mixture was allowed to warm up to room temperature and was stirred overnight. The reaction was quenched with water and cooled with ice. The aqueous phase was extracted with EtOAc (3 \times 25 ml). The combined organic layers

were dried over Na_2SO_4 and evaporated. The residue was purified by semi-preparative HPLC.

Method B: The respective ester derivative was dissolved in a mixture of THF/ H_2O (3:1 v/v, $c=0.4\text{M}$) and was treated with lithium hydroxide monohydrate (2 equiv). The mixture was stirred overnight at room temperature. The solvent was evaporated and the remains were taken up in water, acidified by means of diluted aqueous HCl (1 M), and extracted with EtOAc ($3 \times 25\text{ml}$). The combined organic layers were dried over Na_2SO_4 and evaporated. The residue was used without further purification.

Method C: The respective benzyl-protected hydroxamic acid was dissolved in a mixture of MeOH/THF (1:1 v/v, 10 ml) and treated with Pd/C (10%, 0.05 equiv). The vial was purged with hydrogen and the mixture was hydrogenated (H_2 , 4 bar) for 4–5 h. The mixture was filtered through celite and evaporated under vacuum. The residue was purified by semi-preparative HPLC.

2-[3-(3-Methyl-5-phenyl-1H-pyrazol-4-yl)ethanehydroxamic acid (14a)

The compound was synthesised from *N*-benzyloxy-2-[3-(3-methyl-5-phenyl-1H-pyrazol-4-yl)acetamide (112 mg, 0.35 mmol) and BBr_3 (1 M in DCM, 697 μL , 0.7 mmol) according to method A as described above. Yield: 22 mg (27%); ESI-MS m/z : 232.2 $[\text{M} + \text{H}]^+$; HPLC: rt 6.56 min (>99%); ^1H NMR (400 MHz, DMSO-d_6): δ 2.20 (s, 3H), 3.21 (s, 1.9H), 3.55 (br s, 0.1H), 7.34–7.38 (m, 1H), 7.44 (t, 2H, $^3\text{J}=7.3\text{ Hz}$), 7.65–7.67 (m, 2H), 10.58 (br s, 1H) mixture of *E/Z* isomers; HRMS m/z : 232.1076 $[\text{M} + \text{H}]^+$; calcd for $\text{C}_{12}\text{H}_{14}\text{N}_3\text{O}_2^+$: 232.1081.

2-[3-(3-Benzyl-5-phenyl-1H-pyrazol-4-yl)ethanehydroxamic acid (14b)

The compound was synthesised from *N*-benzyloxy-2-[3-(3-benzyl-5-phenyl-1H-pyrazol-4-yl)acetamide (102 mg, 0.26 mmol) and BBr_3 (1 M in DCM, 770 μL , 0.77 mmol) according to method A as described above. Yield: 24 mg (30%); ESI-MS m/z : 308.3 $[\text{M} + \text{H}]^+$; HPLC: rt 10.43 min (>99%); ^1H NMR (400 MHz, DMSO-d_6): δ 3.21 (s, 1.8H), 3.54 (br s, 0.2H), 3.96 (s, 2H), 7.17–7.22 (m, 1H), 7.26–7.29 (m, 4H), 7.34–7.37 (m, 1H), 7.43 (t, 2H, $^3\text{J}=7.6\text{ Hz}$), 7.66–7.68 (m, 2H), 9.98 (br s, 0.1H), 10.61 (br s, 0.9H) mixture of *E/Z* isomers; HRMS m/z : 308.1389 $[\text{M} + \text{H}]^+$; calcd for $\text{C}_{18}\text{H}_{18}\text{N}_3\text{O}_2^+$: 308.1394.

2-[3-(3-Cyclopentyl-5-phenyl-1H-pyrazol-4-yl)ethanehydroxamic acid (14c)

The compound was synthesised from *N*-benzyloxy-2-[3-(3-cyclopentyl-5-phenyl-1H-pyrazol-4-yl)acetamide (205 mg, 0.55 mmol) and BBr_3 (1 M in DCM, 1.6 ml, 1.64 mmol) according to method A as described above. Yield: 49 mg (31%); ESI-MS m/z : 286.2 $[\text{M} + \text{H}]^+$; HPLC: rt 9.07 min (>99%); ^1H NMR (400 MHz, DMSO-d_6): δ 1.60–1.71 (m, 4H), 1.74–1.78 (m, 2H), 1.93–2.00 (m, 2H), 3.05–3.13 (m, 1H), 3.22 (s, 1.9H), 3.56 (br s, 0.1H), 7.34–7.38 (m, 1H), 7.43 (t, 2H, $^3\text{J}=7.3\text{ Hz}$), 7.67 (d, 2H, $^3\text{J}=7.3\text{ Hz}$), 9.96 (br s, 0.1H), 10.56 (br s, 0.9H) mixture of *E/Z* isomers; HRMS m/z : 286.1545 $[\text{M} + \text{H}]^+$; calcd for $\text{C}_{16}\text{H}_{20}\text{N}_3\text{O}_2^+$: 286.1550.

2-[3-(3-Methoxyphenyl)-5-phenyl-1H-pyrazol-4-yl]ethanehydroxamic acid (14d)

The compound was synthesised from *N*-benzyloxy-2-[3-(3-methoxyphenyl)-5-phenyl-1H-pyrazol-4-yl]acetamide (226 mg, 0.55 mmol)

and Pd/C (30 mg, 0.03 mmol) according to method C as described above. Yield: 145 mg (82%); ESI-MS m/z : 324.3 $[\text{M} + \text{H}]^+$; HPLC: rt 10.69 min (97.9%); ^1H NMR (400 MHz, DMSO-d_6): δ 3.32 (s, 1.8H), 3.63 (br s, 0.2H), 3.81 (s, 3H), 6.95–6.98 (m, 1H), 7.20–7.22 (m, 2H), 7.36–7.42 (m, 2H), 7.47 (t, 2H, $^3\text{J}=7.5\text{ Hz}$), 7.64–7.65 (m, 2H), 10.12 (br s, 0.1H), 10.63 (s, 0.9H) mixture of *E/Z* isomers; HRMS m/z : 324.1341 $[\text{M} + \text{H}]^+$; calcd for $\text{C}_{18}\text{H}_{18}\text{N}_3\text{O}_3^+$: 324.1343.

2-[3-(4-Methoxyphenyl)-5-phenyl-1H-pyrazol-4-yl]ethanehydroxamic acid (14e)

The compound was synthesised from *N*-benzyloxy-2-[3-(4-methoxyphenyl)-5-phenyl-1H-pyrazol-4-yl]acetamide (305 mg, 0.74 mmol) and Pd/C (40 mg, 0.04 mmol) according to method C as described above. Yield: 114 mg (48%); ESI-MS m/z : 324.3 $[\text{M} + \text{H}]^+$; HPLC: rt 10.37 min (97.8%); ^1H NMR (400 MHz, DMSO-d_6): δ 3.29 (s, 1.8H), 3.60 (s, 0.2H), 3.81 (s, 3H), 7.03 (d, 2H, $^3\text{J}=8.7\text{ Hz}$), 7.37–7.41 (m, 1H), 7.46 (t, 2H, $^3\text{J}=7.6\text{ Hz}$), 7.57 (d, 2H, $^3\text{J}=8.7\text{ Hz}$), 7.63–7.65 (m, 2H), 10.08 (br s, 0.1H), 10.60 (s, 0.9H) mixture of *E/Z* isomers; HRMS m/z : 324.1340 $[\text{M} + \text{H}]^+$; calcd for $\text{C}_{18}\text{H}_{18}\text{N}_3\text{O}_3^+$: 324.1343.

2-[3-(1,3-Benzodioxol-5-yl)-5-phenyl-1H-pyrazol-4-yl]ethanehydroxamic acid (14f)

The compound was synthesised from 2-[3-(1,3-benzodioxol-5-yl)-5-phenyl-1H-pyrazol-4-yl]-*N*-benzyloxyacetamide (139 mg, 0.33 mmol) and Pd/C (17 mg, 0.02 mmol) according to method C as described above. Yield: 45 mg (41%); ESI-MS m/z : 338.2 $[\text{M} + \text{H}]^+$; HPLC: rt 10.40 min (98.1%); ^1H NMR (400 MHz, DMSO-d_6): δ 3.29 (s, 1.8H), 3.59 (s, 0.2H), 6.08 (s, 2H), 7.00–7.02 (m, 1H), 7.11–7.14 (m, 1H), 7.20–7.21 (m, 1H), 7.37–7.41 (m, 1H), 7.47 (t, 2H, $^3\text{J}=7.6\text{ Hz}$), 7.61–7.63 (m, 2H), 10.11 (br s, 0.1H), 10.62 (s, 0.9H) mixture of *E/Z* isomers; HRMS m/z : 338.1133 $[\text{M} + \text{H}]^+$; calcd for $\text{C}_{18}\text{H}_{16}\text{N}_3\text{O}_4^+$: 338.1135.

2-[3-(3,4-Dimethoxyphenyl)-5-phenyl-1H-pyrazol-4-yl]ethanehydroxamic acid (14g)

The compound was synthesised from *N*-benzyloxy-2-[3-(3,4-dimethoxyphenyl)-5-phenyl-1H-pyrazol-4-yl]acetamide (120 mg, 0.27 mmol) and Pd/C (14 mg, 0.01 mmol) according to method C as described above. Yield: 49 mg (52%); ESI-MS m/z : 354.3 $[\text{M} + \text{H}]^+$; HPLC: rt 9.95 min (98.6%); ^1H NMR (400 MHz, DMSO-d_6): δ 3.30 (s, 1.8H), 3.61 (br s, 0.2H), 3.80–3.81 (m, 6H), 7.03–7.06 (m, 1H), 7.15–7.17 (m, 1H), 7.23–7.24 (m, 1H), 7.37–7.41 (m, 1H), 7.47 (t, 2H, $^3\text{J}=7.6\text{ Hz}$), 7.66 (d, 2H, $^3\text{J}=7.6\text{ Hz}$), 10.13 (br s, 0.1H), 10.63 (s, 0.9H) mixture of *E/Z* isomers; HRMS m/z : 354.1444 $[\text{M} + \text{H}]^+$; calcd for $\text{C}_{19}\text{H}_{20}\text{N}_3\text{O}_4^+$: 354.1448.

2-[3-(3-Cyanophenyl)-5-phenyl-1H-pyrazol-4-yl]ethanehydroxamic acid (14h)

The compound was synthesised from *N*-benzyloxy-2-[3-(3-cyanophenyl)-5-phenyl-1H-pyrazol-4-yl]acetamide (83 mg, 0.20 mmol) and BBr_3 (1 M in DCM, 610 μL , 0.61 mmol) according to method A as described above. Yield: 25 mg (39%); ESI-MS m/z : 319.2 $[\text{M} + \text{H}]^+$; HPLC: rt 10.48 min (95.6%); ^1H NMR (400 MHz, DMSO-d_6): δ 3.36 (s, 1.8H), 3.66 (br s, 0.2H), 7.42–7.45 (m, 1H), 7.50 (t, 2H, $^3\text{J}=7.6\text{ Hz}$), 7.61–7.64 (m, 2H), 7.66–7.71 (m, 1H), 7.86 (d, 1H, $^3\text{J}=7.7\text{ Hz}$), 8.02 (d, 1H, $^3\text{J}=7.8\text{ Hz}$), 8.12 (s, 1H), 10.69 (s, 0.9H), 10.92 (s, 0.1H) mixture of *E/Z* isomers; HRMS m/z : 319.1186 $[\text{M} + \text{H}]^+$; calcd for $\text{C}_{18}\text{H}_{15}\text{N}_4\text{O}_2^+$: 319.1190.

2-[3-(4-Cyanophenyl)-5-phenyl-1H-pyrazol-4-yl]ethanehydroxamic acid (14i)

The compound was synthesised from *N*-benzyloxy-2-[3-(4-cyanophenyl)-5-phenyl-1H-pyrazol-4-yl]acetamide (84 mg, 0.21 mmol) and BBr_3 (1 M in DCM, 617 μL , 0.62 mmol) according to method A as described above. Yield: 27 mg (42%); ESI-MS m/z : 319.2 $[\text{M} + \text{H}]^+$; HPLC: rt 10.56 min (>99%); ^1H NMR (400 MHz, DMSO-d_6): δ 3.36 (s, 1.8H), 3.67 (br s, 0.2H), 7.42–7.45 (m, 1H), 7.50 (t, 2H, $^3\text{J} = 7.6$ Hz), 7.62 (d, 2H, $^3\text{J} = 7.7$ Hz), 7.88–7.94 (m, 4H), 10.15 (br s, 0.1H), 10.68 (s, 0.9H) mixture of *E/Z* isomers; HRMS m/z : 319.1185 $[\text{M} + \text{H}]^+$; calcd for $\text{C}_{18}\text{H}_{15}\text{N}_4\text{O}_2^+$: 319.1190.

3-[4-[2-(Hydroxyamino)-2-oxo-ethyl]-5-phenyl-1H-pyrazol-3-yl]benzoic acid (14j)

The compound was synthesised from methyl-3-[4-[2-(benzyloxyamino)-2-oxo-ethyl]-5-phenyl-1H-pyrazol-3-yl]benzoate (117 mg, 0.27 mmol) and BBr_3 (1 M in DCM, 2.7 ml, 2.66 mmol) according to method A as described above. Yield: 5 mg (6%); ESI-MS m/z : 338.2 $[\text{M} + \text{H}]^+$; HPLC: rt 9.39 min (95.8%); ^1H NMR (400 MHz, DMSO-d_6): δ 3.35 (s, 1.7H), 3.65 (br s, 0.3H), 7.40–7.43 (m, 1H), 7.49 (t, 2H, $^3\text{J} = 7.6$ Hz), 7.57–7.65 (m, 3H), 7.89 (d, 1H, $^3\text{J} = 7.8$ Hz), 7.96 (d, 1H, $^3\text{J} = 7.8$ Hz), 8.27 (s, 1H), 10.12 (br s, 0.1H), 10.61 (s, 0.9H) mixture of *E/Z* isomers; HRMS m/z : 338.1134 $[\text{M} + \text{H}]^+$; calcd for $\text{C}_{18}\text{H}_{16}\text{N}_3\text{O}_4^+$: 338.1135.

4-[4-[2-(Hydroxyamino)-2-oxo-ethyl]-5-phenyl-1H-pyrazol-3-yl]benzoic acid (14k)

The compound was synthesised from methyl-4-[4-[2-(benzyloxyamino)-2-oxo-ethyl]-5-phenyl-1H-pyrazol-3-yl]benzoate (396 mg, 0.90 mmol) and BBr_3 (1 M in DCM, 9 ml, 8.97 mmol) according to method A as described above. Yield: 16.2 mg (5%); ESI-MS m/z : 338.3 $[\text{M} + \text{H}]^+$; HPLC: rt 9.41 min (95.5%); ^1H NMR (400 MHz, DMSO-d_6): δ 3.67 (br s, 0.2H), 7.41–7.44 (m, 1H), 7.49 (t, 2H, $^3\text{J} = 7.5$ Hz), 7.65 (d, 2H, $^3\text{J} = 7.6$ Hz), 7.79 (d, 2H, $^3\text{J} = 8.1$ Hz), 8.01–8.05 (m, 2H), 8.91 (br s, 0.9H), 9.26 (br s, 0.1H), 10.13 (br s, 0.1H), 10.66 (s, 0.9H), 13.16 (br s, 1H) mixture of *E/Z* isomers; HRMS m/z : 338.1134 $[\text{M} + \text{H}]^+$; calcd for $\text{C}_{18}\text{H}_{16}\text{N}_3\text{O}_4^+$: 338.1135.

2-[3-(4-Chloro-2-fluoro-3-hydroxyphenyl)-5-phenyl-1H-pyrazol-4-yl]ethanehydroxamic acid (14l)

The compound was synthesised from *N*-benzyloxy-2-[3-(4-chloro-2-fluoro-3-methoxyphenyl)-5-phenyl-1H-pyrazol-4-yl]acetamide (80 mg, 0.17 mmol) and BBr_3 (1 M in DCM, 1 ml, 1.03 mmol) according to method A as described above. Yield: 28 mg (45%); ESI-MS m/z : 362.2 $[\text{M} + \text{H}]^+$; HPLC: rt 10.32 min (97.0%); ^1H NMR (400 MHz, DMSO-d_6): δ 3.24 (s, 1.8H), 3.55 (br s, 0.2H), 7.00 (t, 1H, $^3\text{J} = 7.8$ Hz), 7.26–7.29 (m, 1H), 7.38–7.42 (m, 1H), 7.47 (t, 2H, $^3\text{J} = 7.3$ Hz), 7.66 (d, 2H, $^3\text{J} = 7.3$ Hz), 9.92 (br s, 0.1H), 10.45 (br s, 1.9H) mixture of *E/Z* isomers; HRMS m/z : 362.0699 $[\text{M} + \text{H}]^+$; calcd for $\text{C}_{17}\text{H}_{14}\text{ClFN}_3\text{O}_3^+$: 362.0702.

2-[3-(3-Chloro-5-fluoro-4-hydroxyphenyl)-5-phenyl-1H-pyrazol-4-yl]ethanehydroxamic acid (14m)

The compound was synthesised from *N*-benzyloxy-2-[3-(3-chloro-5-fluoro-4-methoxyphenyl)-5-phenyl-1H-pyrazol-4-yl]acetamide (100 mg, 0.21 mmol) and BBr_3 (1 M in DCM, 1.3 ml, 1.29 mmol) according to method A as described above. Yield: 13 mg (17%); ESI-MS m/z : 362.3 $[\text{M} + \text{H}]^+$; HPLC: rt 10.51 min (95.9%); ^1H NMR

(400 MHz, DMSO-d_6): δ 3.30 (s, 1.8H), 3.61 (s, 0.2H), 7.39–7.44 (m, 1H), 7.46–7.52 (m, 4H), 7.60 (d, 2H, $^3\text{J} = 7.3$ Hz), 10.57 (br s, 1H), 10.69 (s, 0.9H), 10.92 (s, 0.1H) mixture of *E/Z* isomers; HRMS m/z : 362.0699 $[\text{M} + \text{H}]^+$; calcd for $\text{C}_{17}\text{H}_{14}\text{ClFN}_3\text{O}_3^+$: 362.0702.

2-[3-(3-Hydroxyisoxazol-5-yl)-5-phenyl-1H-pyrazol-4-yl]ethanehydroxamic acid (14n)

The compound was synthesised from *N*-benzyloxy-2-[3-(3-benzyloxyisoxazol-5-yl)-5-phenyl-1H-pyrazol-4-yl]acetamide (100 mg, 0.21 mmol) and BBr_3 (1 M in DCM, 1.2 ml, 1.25 mmol) according to method A as described above. Yield: 10 mg (16%); ESI-MS m/z : 301.3 $[\text{M} + \text{H}]^+$; HPLC: rt 8.37 min (>99%); ^1H NMR (400 MHz, DMSO-d_6): δ 3.44 (s, 1.8H), 3.76 (s, 0.2H), 6.16–6.25 (m, 1H), 7.43–7.47 (m, 1H), 7.49–7.53 (m, 2H), 7.61–7.63 (m, 2H), 10.08 (br s, 0.1H), 10.63 (s, 0.9H), 11.37 (br s, 1H) mixture of *E/Z* isomers; HRMS m/z : 301.0929 $[\text{M} + \text{H}]^+$; calcd for $\text{C}_{14}\text{H}_{13}\text{N}_4\text{O}_4^+$: 301.0931.

2-[5-Phenyl-3-[3-(trifluoromethyl)-1H-pyrazol-4-yl]-1H-pyrazol-4-yl]ethanehydroxamic acid (14o)

The compound was synthesised from *N*-benzyloxy-2-[3-[1-*tert*-butyl-3-(trifluoromethyl)pyrazol-4-yl]-5-phenyl-1H-pyrazol-4-yl]acetamide (120 mg, 0.24 mmol) and BBr_3 (1 M in DCM, 965 μL , 0.96 mmol) according to method A as described above. Yield: 26 mg (30%); ESI-MS m/z : 352.2 $[\text{M} + \text{H}]^+$; HPLC: rt 9.84 min (97.9%); ^1H NMR (400 MHz, DMSO-d_6): δ 3.21 (s, 1.8H), 3.52 (br s, 0.2H), 7.39–7.42 (m, 1H), 7.48 (t, 2H, $^3\text{J} = 7.7$ Hz), 7.64–7.66 (m, 2H), 8.07 (s, 1H), 10.00 (br s, 0.1H), 10.55 (s, 0.9H), 13.77 (br s, 1H) mixture of *E/Z* isomers; HRMS m/z : 352.1013 $[\text{M} + \text{H}]^+$; calcd for $\text{C}_{15}\text{H}_{13}\text{F}_3\text{N}_5\text{O}_2^+$: 352.1016.

2-[5-Phenyl-3-[3-(1H-tetrazol-5-yl)phenyl]-1H-pyrazol-4-yl]ethanehydroxamic acid (14p)

The compound was synthesised from *N*-benzyloxy-2-[3-[3-[1-(4-methoxyphenyl)methyl]-tetrazol-5-yl]phenyl]-5-phenyl-1H-pyrazol-4-yl]acetamide (188 mg, 0.33 mmol) and BBr_3 (1 M in DCM, 1.3 ml, 1.32 mmol) according to method A as described above. Yield: 38 mg (32%); ESI-MS m/z : 362.1 $[\text{M} + \text{H}]^+$; HPLC: rt 9.47 min (>99%); ^1H NMR (400 MHz, DMSO-d_6): δ 3.40 (s, 1.7H), 3.66 (br s, 0.3H), 7.41–7.45 (m, 1H), 7.51 (t, 2H, $^3\text{J} = 7.5$ Hz), 7.64–7.72 (m, 3H), 7.86–7.88 (m, 1H), 8.04–8.06 (m, 1H), 8.37 (s, 1H), 10.11 (br s, 0.1H), 10.62 (s, 0.9H) mixture of *E/Z* isomers; HRMS m/z : 362.1356 $[\text{M} + \text{H}]^+$; calcd for $\text{C}_{18}\text{H}_{16}\text{N}_7\text{O}_2^+$: 362.1360.

Cis-2-[4-[2-(hydroxyamino)-2-oxo-ethyl]-5-phenyl-1H-pyrazol-3-yl]cyclohexanecarboxylic acid (14q)

The compound was synthesised from *cis*-2-[4-[2-(benzyloxyamino)-2-oxo-ethyl]-5-phenyl-1H-pyrazol-3-yl]cyclohexanecarboxylic acid (147 mg, 0.34 mmol) and BBr_3 (1 M in DCM, 3.4 mL, 3.39 mmol) according to method A as described above. Yield: 2 mg (2%); ESI-MS m/z : 344.2 $[\text{M} + \text{H}]^+$; HPLC: rt 9.01 min (95.6%); ^1H NMR (400 MHz, DMSO-d_6): δ 1.35–1.40 (m, 3H), 1.60–1.75 (m, 3.5H), 1.78–1.87 (m, 0.5H), 1.99–2.07 (m, 1H), 2.18 (br s, 1H), 2.76–2.74 (m, 1H), 3.17–3.30 (m, 2H), 7.33–7.37 (m, 1H), 7.41–7.45 (m, 2H), 7.48–7.50 (m, 0.2H), 7.61–7.62 (m, 1.8H), 10.52 (br s, 0.2H), 10.50 (s, 0.7H) mixture of *E/Z* isomers; HRMS m/z : 344.1599 $[\text{M} + \text{H}]^+$; calcd for $\text{C}_{18}\text{H}_{22}\text{N}_3\text{O}_4^+$: 344.1605.

3-[4-[2-(Hydroxyamino)-2-oxo-ethyl]-5-phenyl-1H-pyrazol-3-yl]cyclohexanecarboxylic acid (14r)

The compound was synthesised from methyl-3-[4-[2-(benzyloxyamino)-2-oxo-ethyl]-5-phenyl-1H-pyrazol-3-yl]cyclohexanecarboxylate (175 mg, 0.39 mmol) and BBr_3 (1 M in DCM, 3.9 mL, 3.91 mmol) according to method A as described above. Yield: 11 mg (8%); ESI-MS m/z : 344.3 $[\text{M} + \text{H}]^+$; HPLC: rt 8.64 min (96.5%); ^1H NMR (400 MHz, DMSO-d_6): 1.26–1.49 (m, 3H), 1.55–1.64 (m, 1H), 1.79–1.85 (m, 2H), 1.92–2.01 (m, 2H), 2.32–2.38 (m, 1H), 2.74–2.78 (m, 1H), 3.22 (s, 2H), 7.33–7.37 (m, 1H), 7.43 (t, 2H, $^3J = 7.4$ Hz), 7.65–7.67 (m, 2H), 9.99 (br s, 0.1H), 10.67 (s, 0.9H) mixture of *E/Z* isomers; HRMS m/z : 344.1598 $[\text{M} + \text{H}]^+$; calcd for $\text{C}_{18}\text{H}_{22}\text{N}_3\text{O}_4^+$: 344.1605.

Trans-4-[4-[2-(hydroxyamino)-2-oxo-ethyl]-5-phenyl-1H-pyrazol-3-yl]cyclohexanecarboxylic acid (14s)

The compound was synthesised from *trans*-methyl-4-[4-[2-(benzyloxyamino)-2-oxo-ethyl]-5-phenyl-1H-pyrazol-3-yl]cyclohexanecarboxylate (85 mg, 0.19 mmol) and BBr_3 (1 M in DCM, 1.9 mL, 1.90 mmol) according to method A as described above. Yield: 8 mg (12%); ESI-MS m/z : 344.3 $[\text{M} + \text{H}]^+$; HPLC: rt 8.69 min (>99%); ^1H NMR (400 MHz, CD_3OD): 1.52–1.73 (m, 4H), 2.07–2.17 (m, 4H), 2.39–2.45 (m, 1H), 2.81–2.87 (m, 1H), 3.42 (s, 1.8H), 3.79 (s, 0.2H), 7.45–7.54 (m, 3H), 7.58–7.59 (m, 0.2H), 7.63–7.66 (m, 1.8H) mixture of *E/Z* isomers; HRMS m/z : 344.1600 $[\text{M} + \text{H}]^+$; calcd for $\text{C}_{18}\text{H}_{22}\text{N}_3\text{O}_4^+$: 344.1605.

Cis-4-[4-[2-(hydroxyamino)-2-oxo-ethyl]-5-phenyl-1H-pyrazol-3-yl]cyclohexanecarboxylic acid (14t)

The compound was synthesised from *cis*-methyl-4-[4-[2-(benzyloxyamino)-2-oxo-ethyl]-5-phenyl-1H-pyrazol-3-yl]cyclohexanecarboxylate (103 mg, 0.23 mmol) and BBr_3 (1 M in DCM, 2.3 mL, 2.30 mmol) according to method A as described above. Yield: 10 mg (13%); ESI-MS m/z : 344.2 $[\text{M} + \text{H}]^+$; HPLC: rt 8.67 min (>99%); ^1H NMR (400 MHz, DMSO-d_6): 1.40–1.66 (m, 5H), 1.83–1.87 (m, 1H), 1.95–2.01 (m, 1H), 2.10–2.13 (m, 1H), 2.19–2.25 (m, 0.5H), 2.60–2.71 (m, 1.5H), 3.19 (s, 1.8H), 3.53 (br s, 0.2H), 7.33–7.36 (m, 1H), 7.40–7.44 (m, 2H), 7.50–7.53 (m, 0.2H), 7.64–7.68 (m, 1.8H), 9.98 (br s, 0.1H), 10.59–10.62 (0.9H) mixture of *E/Z* isomers; HRMS m/z : 344.1598 $[\text{M} + \text{H}]^+$; calcd for $\text{C}_{18}\text{H}_{22}\text{N}_3\text{O}_4^+$: 344.1605.

2-[3,5-Bis(1,3-benzodioxol-5-yl)-1H-pyrazol-4-yl]ethanehydroxamic acid (16a)

The compound was synthesised from *N*-benzyloxy-2-[3,5-bis(1,3-benzodioxol-5-yl)-1H-pyrazol-4-yl]acetamide (290 mg, 0.62 mmol) and Pd/C (33 mg, 0.03 mmol) according to method C as described above. Yield: 30 mg (13%); ESI-MS m/z : 382.3 $[\text{M} + \text{H}]^+$; HPLC: rt 10.72 min (95.4%); ^1H NMR (400 MHz, DMSO-d_6): δ 3.26 (s, 1.9H), 3.56 (br s, 0.1H), 6.08 (s, 4H), 6.99–7.01 (m, 2H), 7.08–7.10 (m, 2H), 7.16–7.17 (m, 2H), 10.12 (br s, 0.1H), 10.63 (s, 0.9H) mixture of *E/Z* isomers; HRMS m/z : 382.1028 $[\text{M} + \text{H}]^+$; calcd for $\text{C}_{19}\text{H}_{16}\text{N}_3\text{O}_6^+$: 382.1034.

3-[3-(3-Carboxyphenyl)-4-[2-(hydroxyamino)-2-oxo-ethyl]-1H-pyrazol-5-yl]benzoic acid (16b)

The compound was synthesised from methyl-3-[4-[2-(benzyloxyamino)-2-oxo-ethyl]-3-(3-methoxycarbonylphenyl)-1H-pyrazol-5-yl]benzoate (150 mg, 0.30 mmol) and BBr_3 (1 M in DCM, 4.5 mL,

4.50 mmol) according to method A as described above. Yield: 3 mg (3%); ESI-MS m/z : 382.3 $[\text{M} + \text{H}]^+$; HPLC: rt 8.72 min (>99%); ^1H NMR (400 MHz, DMSO-d_6): δ 3.37 (s, 1.8H), 3.66 (s, 0.2H), 7.61 (t, 2H, $^3J = 7.8$ Hz), 7.87–7.89 (m, 2H), 7.96–7.98 (m, 2H), 8.20–8.25 (m, 2H), 10.13 (br s, 0.1H), 10.61 (s, 0.9H) mixture of *E/Z* isomers; HRMS m/z : 382.1036 $[\text{M} + \text{H}]^+$; calcd for $\text{C}_{19}\text{H}_{16}\text{N}_3\text{O}_6^+$: 382.1034.

4-[3-(4-Carboxyphenyl)-4-[2-(hydroxyamino)-2-oxo-ethyl]-1H-pyrazol-5-yl]benzoic acid (16c)

The compound was synthesised from methyl-4-[4-[2-(benzyloxyamino)-2-oxo-ethyl]-3-(4-methoxycarbonylphenyl)-1H-pyrazol-5-yl]benzoate (100 mg, 0.20 mmol) and BBr_3 (1 M in DCM, 2 mL, 2 mmol) according to method A as described above. Yield: 3 mg (3%); ESI-MS m/z : 382.2 $[\text{M} + \text{H}]^+$; HPLC: rt 8.43 min (96.4%); ^1H NMR (400 MHz, CD_3OD): δ 3.49 (s, 2H), 7.74–7.76 (m, 4H), 8.09–8.14 (m, 4H); HRMS m/z : 382.1030 $[\text{M} + \text{H}]^+$; calcd for $\text{C}_{19}\text{H}_{16}\text{N}_3\text{O}_6^+$: 382.1034.

2-[3,5-Bis(4-chloro-2-fluoro-3-hydroxyphenyl)-1H-pyrazol-4-yl]ethanehydroxamic acid (16d)

The compound was synthesised from *N*-benzyloxy-2-[3,5-bis(4-chloro-2-fluoro-3-methoxyphenyl)-1H-pyrazol-4-yl]acetamide (50 mg, 0.09 mmol) and BBr_3 (1 M in DCM, 912 μL , 0.91 mmol) according to method A as described above. Yield: 4 mg (11%); ESI-MS m/z : 430.3 $[\text{M} + \text{H}]^+$; HPLC: rt 10.40 min (96.8%); ^1H NMR (400 MHz, DMSO-d_6): δ 3.15 (s, 1.8H), 3.47 (br s, 0.2H), 6.99–7.03 (m, 2H), 7.26–7.29 (m, 2H), 9.76 (br s, 0.1H), 10.31 (s, 0.9H), 10.50 (br s, 2H) mixture of *E/Z* isomers; HRMS m/z : 430.0164 $[\text{M} + \text{H}]^+$; calcd for $\text{C}_{17}\text{H}_{12}\text{Cl}_2\text{F}_2\text{N}_3\text{O}_4^+$: 430.0167.

3-[3-(1,3-Benzodioxol-5-yl)-4-[2-(hydroxyamino)-2-oxo-ethyl]-1H-pyrazol-5-yl]benzoic acid (16e)

The compound was synthesised from methyl-3-[3-(1,3-benzodioxol-5-yl)-4-[2-(benzyloxyamino)-2-oxo-ethyl]-1H-pyrazol-5-yl]benzoate (180 mg, 0.37 mmol) and lithium hydroxide monohydrate (31 mg, 0.74 mmol) according to method B and C as described above. Yield: 90 mg (69%); ESI-MS m/z : 382.3 $[\text{M} + \text{H}]^+$; HPLC: rt 9.63 min (>99%); ^1H NMR (400 MHz, DMSO-d_6): δ 3.32 (s, 1.8H), 3.61 (br s, 0.2H), 6.09 (s, 2H), 7.02–7.04 (m, 1H), 7.10–7.13 (m, 1H), 7.19–7.20 (m, 1H), 7.58 (t, 1H, $^3J = 7.7$ Hz), 7.84–7.86 (m, 1H), 7.94–7.96 (m, 1H), 8.18–8.24 (m, 1H), 10.13 (br s, 0.1H), 10.62 (s, 0.9H) mixture of *E/Z* isomers; HRMS m/z : 382.1029 $[\text{M} + \text{H}]^+$; calcd for $\text{C}_{19}\text{H}_{16}\text{N}_3\text{O}_6^+$: 382.1034.

4-[3-(1,3-Benzodioxol-5-yl)-4-[2-(hydroxyamino)-2-oxo-ethyl]-1H-pyrazol-5-yl]benzoic acid (16f)

The compound was synthesised from methyl-4-[3-(1,3-benzodioxol-5-yl)-4-[2-(benzyloxyamino)-2-oxo-ethyl]-1H-pyrazol-5-yl]benzoate (160 mg, 0.33 mmol) and lithium hydroxide monohydrate (28 mg, 0.66 mmol) according to method B and C as described above. Yield: 8 mg (10%); ESI-MS m/z : 382.2 $[\text{M} + \text{H}]^+$; HPLC: rt 9.68 min (>99%); ^1H NMR (400 MHz, DMSO-d_6): δ 3.33 (s, 1.8H), 3.63 (br s, 0.2H), 6.09 (s, 2H), 7.02–7.04 (m, 1H), 7.12–7.14 (m, 1H), 7.21–7.22 (m, 1H), 7.75–7.77 (m, 2H), 8.00–8.02 (m, 2H), 10.14 (br s, 0.1H), 10.66 (s, 0.9H) mixture of *E/Z* isomers; HRMS m/z : 382.1030 $[\text{M} + \text{H}]^+$; calcd for $\text{C}_{19}\text{H}_{16}\text{N}_3\text{O}_6^+$: 382.1034.

3-[3-(4-Carboxyphenyl)-4-[2-(hydroxyamino)-2-oxo-ethyl]-1H-pyrazol-5-yl]benzoic acid (16g)

The compound was synthesised from methyl-3-[4-[2-(benzyloxyamino)-2-oxo-ethyl]-3-(4-methoxycarbonylphenyl)-1H-pyrazol-5-yl]benzoate (50 mg, 0.10 mmol) and BBr_3 (1 M in DCM, 1.5 mL, 1.50 mmol) according to method A described above. Yield: 3 mg (7%); ESI-MS m/z : 382.3 $[\text{M} + \text{H}]^+$; HPLC: rt 8.64 min (>99%); ^1H NMR (400 MHz, CD_3OD): δ 3.49 (s, 1.8H), 3.82 (br s, 0.2H), 7.60 (t, 1H, $^3J = 7.8$ Hz), 7.75–7.77 (m, 2H), 7.87–7.89 (m, 1H), 8.07–8.14 (m, 3H), 8.30 (s, 1H) mixture of *E/Z* isomers; HRMS m/z : 382.1033 $[\text{M} + \text{H}]^+$; calcd for $\text{C}_{19}\text{H}_{16}\text{N}_3\text{O}_6^+$: 382.1034.

4-[5-(4-Chloro-2-fluoro-3-hydroxy-phenyl)-4-[2-(hydroxyamino)-2-oxo-ethyl]-1H-pyrazol-3-yl]benzoic acid (16h)

The compound was synthesised from methyl-4-[4-[2-(benzyloxyamino)-2-oxo-ethyl]-5-(4-chloro-2-fluoro-3-methoxy-phenyl)-1H-pyrazol-3-yl]benzoate (90 mg, 0.17 mmol) and BBr_3 (1 M in DCM, 2.1 mL, 2.06 mmol) according to method A described above. Yield: 4 mg (5%); ESI-MS m/z : 406.3 $[\text{M} + \text{H}]^+$; HPLC: rt 9.63 min (>99%); ^1H NMR (400 MHz, MeCN-d_3): δ 3.40 (s, 1.8H), 3.74 (br s, 0.2H), 6.97–7.01 (m, 1H), 7.21–7.24 (m, 1H), 7.76–7.78 (m, 2H), 8.11–8.13 (m, 2H) mixture of *E/Z* isomers; HRMS m/z : 406.0597 $[\text{M} + \text{H}]^+$; calcd for $\text{C}_{18}\text{H}_{14}\text{ClFN}_3\text{O}_5^+$: 406.0601.

3-[5-(4-Chloro-2-fluoro-3-hydroxy-phenyl)-4-[2-(hydroxyamino)-2-oxo-ethyl]-1H-pyrazol-3-yl]benzoic acid (16i)

The compound was synthesised from methyl-3-[4-[2-(benzyloxyamino)-2-oxo-ethyl]-5-(4-chloro-2-fluoro-3-methoxy-phenyl)-1H-pyrazol-3-yl]benzoate (30 mg, 0.06 mmol) and BBr_3 (1 M in DCM, 687 μL , 0.69 mmol) according to method A described above. Yield: 4 mg (16%); ESI-MS m/z : 406.3 $[\text{M} + \text{H}]^+$; HPLC: rt 9.55 min (95.3%); ^1H NMR (400 MHz, DMSO-d_6): δ 3.26 (s, 2H), 6.97–7.01 (m, 1H), 7.28–7.30 (m, 1H), 7.57–7.61 (m, 1H), 7.90–7.92 (m, 1H), 7.95–7.97 (m, 1H), 8.21–8.27 (m, 1H), 9.95 (br s, 0.1H), 10.45 (s, 0.7H), 10.53 (br s, 0.5H) mixture of *E/Z* isomers; HRMS m/z : 406.0597 $[\text{M} + \text{H}]^+$; calcd for $\text{C}_{18}\text{H}_{14}\text{ClFN}_3\text{O}_5^+$: 406.0601.

3-[5-(3-Chloro-5-fluoro-4-hydroxy-phenyl)-4-[2-(hydroxyamino)-2-oxo-ethyl]-1H-pyrazol-3-yl]benzoic acid (16j)

The compound was synthesised from methyl-3-[4-[2-(benzyloxyamino)-2-oxo-ethyl]-5-(3-chloro-5-fluoro-4-methoxy-phenyl)-1H-pyrazol-3-yl]benzoate (90 mg, 0.17 mmol) and BBr_3 (1 M in DCM, 2.1 mL, 2.06 mmol) according to method A described above. Yield: 18 mg (26%); ESI-MS m/z : 406.3 $[\text{M} + \text{H}]^+$; HPLC: rt 9.55 min (97.6%); ^1H NMR (400 MHz, DMSO-d_6): δ 3.33 (s, 1.8H), 3.63 (br s, 0.2H), 7.47–7.52 (m, 2H), 7.60 (t, 1H, $^3J = 7.8$ Hz), 7.83–7.84 (m, 1H), 7.96–7.98 (m, 1H), 8.16–8.22 (m, 1H), 10.19 (br s, 0.1H), 10.62–10.68 (m, 1.9H) mixture of *E/Z* isomers; HRMS m/z : 406.0593 $[\text{M} + \text{H}]^+$; calcd for $\text{C}_{18}\text{H}_{14}\text{ClFN}_3\text{O}_5^+$: 406.0601.

3-[4-[2-(Hydroxyamino)-2-oxo-ethyl]-3-[cis-2-carboxycyclohexyl]-1H-pyrazol-5-yl]benzoic acid (16k)

The compound was synthesised from *cis*-2-[4-[2-(benzyloxyamino)-2-oxo-ethyl]-5-(3-methoxycarbonylphenyl)-1H-pyrazol-3-yl]cyclohexanecarboxylic acid (154 mg, 0.31 mmol) and lithium hydroxide monohydrate (26 mg, 0.63 mmol) according to method B and C as described above. Yield: 37 mg (36%); ESI-MS m/z : 388.3 $[\text{M} + \text{H}]^+$; HPLC: rt 8.77 min (96.5%); ^1H NMR (400 MHz, DMSO-d_6): δ 1.37–

1.39 (m, 2H), 1.63–1.73 (m, 4H), 2.08–2.18 (m, 2H), 2.68–2.76 (m, 1H), 3.20–3.29 (m, 3H), 7.56 (t, 1H, $^3J = 7.7$ Hz), 7.89–7.93 (m, 2H), 8.23 (s, 1H), 10.03 (br s, 0.2H), 10.62 (s, 0.8H) mixture of *E/Z* isomers; HRMS m/z : 388.1499 $[\text{M} + \text{H}]^+$; calcd for $\text{C}_{19}\text{H}_{22}\text{N}_3\text{O}_6^+$: 388.1503.

3-[3-(Trans-4-Carboxycyclohexyl)-4-[2-(hydroxyamino)-2-oxo-ethyl]-1H-pyrazol-5-yl]benzoic acid (16l)

The compound was synthesised from methyl-3-[4-[2-(benzyloxyamino)-2-oxo-ethyl]-3-(*trans*-4-methoxycarbonylcyclohexyl)-1H-pyrazol-5-yl]benzoate (216 mg, 0.43 mmol) and BBr_3 (1 M in DCM, 8.1 mL, 8.11 mmol) according to method A described above. Yield: 2 mg (1%); ESI-MS m/z : 388.3 $[\text{M} + \text{H}]^+$; HPLC: rt 7.95 min (>99%); ^1H NMR (400 MHz, CD_3OD): 1.43–1.73 (m, 4H), 2.04–2.16 (m, 4H), 2.38–2.44 (m, 1H), 2.78–2.83 (m, 1H), 3.41 (s, 1.4H), 3.67 (s, 0.6H), 7.59 (t, 1H, $^3J = 7.6$ Hz), 7.88–7.93 (m, 1H), 8.07–8.09 (m, 1H), 8.29 (s, 1H) mixture of *E/Z* isomers; HRMS m/z : 388.1501 $[\text{M} + \text{H}]^+$; calcd for $\text{C}_{19}\text{H}_{22}\text{N}_3\text{O}_6^+$: 388.1503.

3-[3-(Cis-4-Carboxycyclohexyl)-4-[2-(hydroxyamino)-2-oxo-ethyl]-1H-pyrazol-5-yl]benzoic acid (16m)

The compound was synthesised from methyl-3-[4-[2-(benzyloxyamino)-2-oxo-ethyl]-3-(*cis*-4-methoxycarbonylcyclohexyl)-1H-pyrazol-5-yl]benzoate (185 mg, 0.37 mmol) and BBr_3 (1 M in DCM, 7.0 mL, 6.95 mmol) according to method A described above. Yield: 2 mg (2%); ESI-MS m/z : 388.3 $[\text{M} + \text{H}]^+$; HPLC: rt 8.00 min (95.2%); ^1H NMR (400 MHz, CD_3OD): δ 1.57–1.73 (m, 4H), 2.04–2.15 (m, 4H), 2.38–2.48 (m, 1H), 2.77–2.83 (m, 1H), 3.41 (s, 1.7H), 3.66 (s, 0.3H), 7.58 (t, 1H, $^3J = 7.6$ Hz), 7.88–7.90 (m, 1H), 8.06–8.08 (m, 1H), 8.29 (s, 1H) mixture of *E/Z* isomers; HRMS m/z : 388.1502 $[\text{M} + \text{H}]^+$; calcd for $\text{C}_{19}\text{H}_{22}\text{N}_3\text{O}_6^+$: 388.1503.

General methods for the synthesis of *N*-substituted 3,5-diphenylpyrazole derivatives 19a–f, 20, 24a–c

Method A: The respective diphenylpyrazole (1 equiv) was dissolved in DMF (5 ml), cooled down to 0 °C and treated with NaH (60% dispersion in mineral oil, 1.2–1.5 equiv). After 30 min the mixture was allowed to warm up to room temperature and stirred overnight. The reaction mixture was quenched with water and extracted with EtOAc (3 × 25 ml). The combined organic layers were dried over Na_2SO_4 and evaporated. The residue was purified by flash chromatography (silica, heptane/EtOAc).

Method B: The respective diphenylpyrazole (1 equiv) was dissolved in DCM ($c = 0.1$ M) and the respective boronic acid (2 equiv), triethylamine (2 equiv), $\text{Cu}(\text{OAc})_2$ (1.5 equiv), and molecular sieve (3 Å) were added. The mixture was stirred at room temperature and under atmospheric oxygen. After 72 h the mixture was filtered through celite and evaporated. The residue was purified by flash chromatography (silica, heptane/EtOAc).

General method for the synthesis of hydroxamic acids from carboxylic acid esters 21a, 21e–i, 22

The respective ester derivative (1 equiv) was dissolved in dry MeOH (5 ml) and treated with NaOCH_3 (5 N, 6 equiv) and hydroxylamine hydrochloride (3 equiv). The mixture was heated at 80 °C for 10 min in a microwave. After cooling, the volatiles were evaporated. The remains were taken up in a small amount of water and the pH was adjusted to ~8 by means of diluted HCl (1 M). The

aqueous layer was extracted with EtOAc (3 × 25 ml), the combined organic layers were dried over Na₂SO₄, filtered, and evaporated to dryness. The residue was purified by semi-preparative HPLC.

2-(1-Methyl-3,5-diphenyl-pyrazol-4-yl)ethanehydroxamic acid (21a)

The compound was synthesised from methyl-2-(1-methyl-3,5-diphenyl-pyrazol-4-yl)acetate (210 mg, 0.69 mmol), NaOCH₃ (5 N, 823 μL, 4.11 mmol) and hydroxylamine hydrochloride (143 mg, 2.06 mmol). Yield: 96 mg (45%); ESI-MS *m/z*: 308.2 [M + H]⁺; HPLC: rt 11.55 min (>99%); ¹H NMR (400 MHz, DMSO-*d*₆): δ 3.14 (s, 1.8H), 3.45 (s, 0.2H), 3.77 (s, 3H), 7.33–7.37 (m, 1H), 7.42 (t, 2H, ³J = 7.5 Hz), 7.47–7.57 (m, 5H), 7.64–7.67 (m, 2H), 10.00 (s, 0.1H), 10.45 (s, 0.9H) mixture of *E/Z* isomers; HRMS *m/z*: 308.1407 [M + H]⁺; calcd for C₁₈H₁₈N₃O₂⁺: 308.1394.

2-(1-Benzyl-3,5-diphenyl-pyrazol-4-yl)ethanehydroxamic acid (21e)

The compound was synthesised from methyl-2-(1-benzyl-3,5-diphenyl-pyrazol-4-yl)acetate (230 mg, 0.60 mmol), NaOCH₃ (5 N, 722 μL, 3.61 mmol) and hydroxylamine hydrochloride (125 mg, 1.80 mmol). Yield: 81 mg (35%); ESI-MS *m/z*: 384.3 [M + H]⁺, 406.2 [M + Na]⁺; HPLC: rt 15.63 min (>99%); ¹H NMR (400 MHz, DMSO-*d*₆): 3.18 (s, 1.8H), 3.47 (s, 0.2H), 5.28 (s, 2H), 7.01–7.04 (m, 2H), 7.22–7.31 (m, 3H), 7.22–7.31 (m, 3H); 7.34–7.44 (m, 5H), 7.47–7.51 (m, 3H), 7.8–7.70 (m, 2H), 9.97 (s, 0.1H), 10.45 (s, 0.9H) mixtures of *E/Z* isomers; HRMS *m/z*: 384.1726 [M + H]⁺; calcd for C₂₄H₂₂N₃O₂⁺: 384.1707.

2-[1-(1,3-Benzodioxol-5-ylmethyl)-3,5-diphenyl-pyrazol-4-yl]ethanehydroxamic acid (21f)

The compound was synthesised from methyl-2-[1-(1,3-benzodioxol-5-yl-methyl)-3,5-diphenyl-pyrazol-4-yl]acetate (305 mg, 0.72 mmol), NaOCH₃ (858 μL, 4.29 mmol) and hydroxylamine hydrochloride (149 mg, 2.15 mmol). Yield: 161 mg (53%); ESI-MS *m/z*: 428.4 [M + H]⁺; HPLC: rt 15.33 min (>99%); ¹H NMR (400 MHz, DMSO-*d*₆): 3.15 (s, 1.8H), 3.46 (s, 0.2H), 5.17 (s, 2H), 5.97 (s, 2H), 6.47–6.49 (m, 1H), 6.56–6.57 (m, 1H), 6.79–6.81 (m, 1H), 7.34–7.44 (m, 5H), 7.48–7.53 (m, 3H), 7.58–7.59 (m, 0.2H), 7.66–7.69 (m, 1.8H), 9.96 (s, 0.1H), 10.44 (s, 0.9H) mixture of *E/Z* isomers; HRMS *m/z*: 428.1601 [M + H]⁺; calcd for C₂₅H₂₂N₃O₄⁺: 428.1605.

3-[[4-[2-(Hydroxyamino)-2-oxo-ethyl]-3,5-diphenyl-pyrazol-1-yl]methyl]benzoic acid (21g)

The compound was synthesised from 3-[[4-(2-methoxy-2-oxo-ethyl)-3,5-diphenyl-pyrazol-1-yl]methyl]benzoic acid (311 mg, 0.73 mmol), NaOCH₃ (876 μL, 4.38 mmol) and hydroxylamine hydrochloride (152 mg, 2.19 mmol). Yield: 16 mg (5%); ESI-MS *m/z*: 428.2 [M + H]⁺, 450.2 [M + Na]⁺; HPLC: rt 12.88 min (>99%); ¹H NMR (400 MHz, DMSO-*d*₆): 3.17 (s, 1.8H), 3.47 (s, 0.2H), 5.34 (s, 2H), 7.23–7.25 (m, 1H), 7.35–7.50 (m, 9H), 7.58–7.60 (m, 0.3H), 7.67–7.69 (m, 2.7H), 7.81–7.83 (m, 1H), 9.96 (s, 0.1H), 10.45 (s, 0.9H) mixture of *E/Z* isomers; HRMS *m/z*: 428.1599 [M + H]⁺; calcd for C₂₅H₂₂N₃O₄⁺: 428.1605.

4-[[4-[2-(Hydroxyamino)-2-oxo-ethyl]-3,5-diphenyl-pyrazol-1-yl]methyl]benzoic acid (21h)

The compound was synthesised from 4-[[4-(2-methoxy-2-oxo-ethyl)-3,5-diphenyl-pyrazol-1-yl]methyl]benzoic acid (400 mg, 0.94 mmol), NaOCH₃ (1.1 ml, 5.63 mmol) and hydroxylamine hydrochloride (196 mg, 2.81 mmol). Yield: 130 mg (32%); ESI-MS *m/z*: 428.2 [M + H]⁺; HPLC: rt 12.69 min (>99%); ¹H NMR (400 MHz, DMSO-*d*₆): δ 3.18 (s, 1.8H), 3.48 (s, 0.2H), 5.35 (s, 2H), 7.13–7.15 (m, 2H), 7.35–7.49 (m, 8H), 7.59–7.61 (m, 0.2H), 7.68–7.69 (m, 1.8H), 7.85 (t, 2H, ³J = 8.2 Hz), 9.98 (s, 0.1H), 10.45 (s, 0.9H), 12.90 (br s, 1H) mixture of *E/Z* isomers; HRMS *m/z*: 428.1600 [M + H]⁺; calcd for C₂₅H₂₂N₃O₄⁺: 428.1605.

2-[1-[(4-Chloro-2-fluoro-3-hydroxy-phenyl)methyl]-3,5-diphenyl-pyrazol-4-yl]ethanehydroxamic acid (21i)

The compound was synthesised from methyl-2-[1-[(4-chloro-2-fluoro-3-methoxy-phenyl)methyl]-3,5-diphenyl-pyrazol-4-yl]acetate (300 mg, 0.65 mmol), NaOCH₃ (774 μL, 3.87 mmol) and hydroxylamine hydrochloride (135 mg, 1.94 mmol). The final deprotection of the phenol was accomplished by treatment with BBr₃. Briefly, the compound was dissolved in DCM (5 ml) in a sealed flask under argon atmosphere. The solution was cooled to 0 °C and treated with BBr₃ (1 M in DCM, 3 equiv). The mixture was allowed to warm up to room temperature and was stirred overnight. The reaction was quenched with water and cooled with ice. The aqueous phase was extracted with EtOAc (3 × 25 ml). The combined organic layers were dried over Na₂SO₄ and evaporated. The residue was purified by semi-preparative HPLC. Yield: 142 mg (54%); ESI-MS *m/z*: 452.2 [M + H]⁺; HPLC: rt 14.75 min (98.4%); ¹H NMR (400 MHz, DMSO-*d*₆): δ 3.15 (s, 1.8H), 3.46 (s, 0.2H), 5.27 (s, 2H), 6.42–6.46 (m, 1H), 7.11–7.13 (m, 1H), 7.34–7.44 (m, 5H), 7.49–7.53 (m, 3H), 7.57–7.58 (m, 0.2H), 7.65–7.67 (m, 1.8H), 9.97 (s, 0.1H), 10.36 (br s, 1H), 10.44 (s, 0.9H) mixture of *E/Z* isomers; HRMS *m/z*: 452.1165 [M + H]⁺; calcd for C₂₄H₂₀ClFN₃O₃⁺: 452.1172.

3-[1-[(4-Chloro-2-fluoro-3-hydroxy-phenyl)methyl]-3,5-diphenyl-pyrazol-4-yl]propanehydroxamic acid (22)

The compound was synthesised from methyl-3-[1-[(4-chloro-2-fluoro-3-methoxy-phenyl)methyl]-3,5-diphenyl-pyrazol-4-yl]propanoate (250 mg, 0.52 mmol), NaOCH₃ (626 μL, 3.13 mmol) and hydroxylamine hydrochloride (109 mg, 1.57 mmol). The final deprotection of the phenol was accomplished by treatment with BBr₃. Briefly, the compound was dissolved in DCM (5 ml) in a sealed flask under argon atmosphere. The solution was cooled to 0 °C and treated with BBr₃ (1 M in DCM, 3 equiv). The mixture was allowed to warm up to room temperature and was stirred overnight. The reaction was quenched with water and cooled with ice. The aqueous phase was extracted with EtOAc (3 × 25 ml). The combined organic layers were dried over Na₂SO₄ and evaporated. The residue was purified by semi-preparative HPLC. Yield: 56 mg (23%); ESI-MS *m/z*: 466.2 [M + H]⁺; HPLC: rt 15.28 min (>99%); ¹H NMR (400 MHz, DMSO-*d*₆): δ 1.95–1.97 (m, 1.8H), 2.23–2.27 (m, 0.2H), 2.72–2.75 (m, 2H), 5.21 (s, 2H), 6.36 (t, 1H, ³J = 7.9 Hz), 7.10 (d, 1H, ³J = 8.6 Hz), 7.36–7.38 (m, 3H), 7.45 (t, 2H, ³J = 7.5 Hz), 7.49–7.53 (m, 3H), 7.68 (d, 2H, ³J = 7.5 Hz), 9.75 (s, 0.1H), 10.26 (s, 0.9H), 10.36 (s, 1H) mixture of *E/Z* isomers; HRMS *m/z*: 466.1325 [M + H]⁺; calcd for C₂₅H₂₂ClFN₃O₃⁺: 466.1328.

General method for deprotection of trityl-protected hydroxamic acid derivatives 21b–d

The respective trityl-protected hydroxamic acid derivative (1 equiv) was treated with TFA/DCM (1:1 v/v, 5 ml) and triisopropylsilane (1.5 equiv). The mixture was stirred for 3 h at room temperature. The volatiles were evaporated and the residue was purified by semi-preparative HPLC.

2-(1,3,5-Triphenylpyrazol-4-yl)ethanehydroxamic acid (21b)

The compound was synthesised from 2-(1,3,5-triphenylpyrazol-4-yl)-*N*-trityloxy-acetamide (150 mg, 0.25 mmol). Yield: 50 mg (55%); ESI-MS: m/z 370.3 $[M + H]^+$, 392.2 $[M + Na]^+$; HPLC: rt 15.49 min (>99%); 1H NMR (400 MHz, DMSO- d_6): δ 3.24 (s, 1.8H), 3.54 (s, 0.2H), 7.28–7.42 (m, 11H), 7.45–7.49 (m, 2H), 7.66–7.68 (m, 0.2H), 7.74–7.76 (m, 1.8H), 10.06 (s, 0.1H), 10.53 (s, 0.9H) mixture of *E/Z* isomers; HRMS m/z : 370.1569 $[M + H]^+$; calcd for $C_{23}H_{20}N_3O_2^+$: 370.1550.

3-[4-[2-(Hydroxyamino)-2-oxo-ethyl]-3,5-diphenyl-pyrazol-1-yl]benzoic acid (21c)

The compound was synthesised from *tert*-butyl-3-(4-(2-oxo-2-((trityloxy)amino)ethyl)-3,5-diphenyl-1H-pyrazol-1-yl)benzoate (210 mg, 0.30 mmol). Yield: 45 mg (39%); ESI-MS m/z : 414.3 $[M + H]^+$; HPLC: rt 13.09 min (>99%); 1H NMR (400 MHz, DMSO- d_6): δ 3.25 (s, 1.8H), 3.55 (s, 0.2H), 7.28–7.35 (m, 2H), 7.40–7.50 (m, 8H), 7.67–7.69 (m, 0.2H), 7.75–7.76 (m, 1.8H), 7.83–7.86 (m, 1H), 7.89 (s, 1H), 10.08 (s, 0.1H), 10.53 (s, 0.9H) mixture of *E/Z* isomers; HRMS m/z : 414.1468 $[M + H]^+$; calcd for $C_{24}H_{20}N_3O_4^+$: 414.1448.

4-[4-[2-(Hydroxyamino)-2-oxo-ethyl]-3,5-diphenyl-pyrazol-1-yl]benzoic acid (21d)

The compound was synthesised from *tert*-butyl-4-(4-(2-oxo-2-((trityloxy)amino)ethyl)-3,5-diphenyl-1H-pyrazol-1-yl)benzoate (200 mg, 0.28 mmol). Yield: 55 mg (48%); ESI-MS m/z : 414.2 $[M + H]^+$; HPLC: rt 13.08 min (>99%); 1H NMR (400 MHz, DMSO- d_6): δ 3.24 (s, 1.8H), 3.55 (s, 0.2H), 7.28–7.52 (m, 10H), 7.68–7.79 (m, 2H), 7.90–7.92 (m, 2H), 10.09 (s, 0.1H), 10.55 (s, 0.9H) mixture of *E/Z* isomers; HRMS m/z : 414.1466 $[M + H]^+$; calcd for $C_{24}H_{20}N_3O_4^+$: 414.1448.

Docking

The docking experiments were performed with GOLD⁵⁰ in combination with the HERMES visualiser (Cambridge Crystallographic Data Centre, version 2020.1). For the target meprin β the pdb structure PDB ID: 7AQ1 was employed⁴⁰. Only chain A and the corresponding zinc ion were used (monomer). For meprin α the recently reported homology model was utilised³⁹. The active site was defined by the zinc ion and a radius of 15 Å. The ligands were used in their deprotonated forms. For each compound, 20 docking runs were performed and scored with ChemScore. The search efficacy was set to 100%. The docking was carried out with a scaffold match constraint to place the ligand onto a given scaffold location within the binding site. The hydroxamic acid substructure of the co-crystallized ligand (PDB ID: 7AQ1) was used as a template for this purpose. Compound **14m** was docked in the rigid conformation of meprin α and β . For compound **21i** and **22** the side chains of the respective amino acids Y¹⁸⁷ and R²⁴² in S1- and S1'-binding site of meprin α were specified as flexible upon docking. The allowed rotamers are defined from a rotamer

library⁵². Docking results were visualised using Molecular Operating Environment (MOE, Chemical Computing Group, version 2019.01)⁵³.

Enzymatic assays

Recombinant human meprin β was expressed in yeast and characterised as previously described⁵⁴. Recombinant human meprin α was expressed and purified from insect cells (S2) and characterised analogously⁵⁵. MMP2, 9, 13, ADAM10, and 17 were purchased from a commercial vendor (R&D systems). MMPs were activated prior to measurement by APMA (*p*-aminophenylmercuric acetate) treatment according to manufacturer's instructions.

The determination of enzymatic activity was based on the cleavage of internally quenched peptide substrates (see Supporting Information). A typical assay of 100 μ L total volume measured in black 96 half area well plates consisted of 40 μ L buffer, 20 μ L enzyme at a final concentration of 2e-10 M for meprin α and 3e-11 M for meprin β , 20 μ L substrate, and 20 μ L inhibitor solution (in buffer, 2% DMSO). Enzymatic activity of ADAMs was measured in 384 well plates with 50 μ L total assay volume consisting of 30 μ L enzyme in buffer, 10 μ L inhibitor, and 10 μ L substrate. To ensure reproducibility, the parameters were determined at least in duplicates independently on separate days. For IC₅₀ values the influence of 11 or 14 inhibitor concentrations ranging from 0 to 1e-4 M on the enzymatic activity was investigated in the presence of the respective substrate concentration. Initial velocities were determined and converted into concentration units applying a standard curve obtained after the complete conversion of different substrate concentrations under assay conditions. All measurements were performed using a fluorescence plate reader (FLUOstar OPTIMA, BMG Labtech) at 30 °C. Depending on the substrates the excitation/emission wavelength was 340/490 nm for enzymatic assays regarding meprin and 340/410 nm for enzymatic assays regarding MMPs and ADAMs. The kinetic data was evaluated using GraphPad Prism (version 5.04, GraphPad Software, San Diego, California USA). Kinetic parameters of inhibition ($K_i^{(app)}$) were determined using Morrison's equation⁵⁶:

$$\frac{v_i}{v_0} = 1 - \frac{E_0 + I_0 + K_i^{(app)} - \sqrt{(E_0 + I_0 + K_i^{(app)})^2 - 4 \cdot E_0 \cdot I_0}}{2 \cdot E_0}$$

Cell viability assay

Cell viability was assessed in human hepatocellular carcinoma cell line Hep-G2 and in human neuroblastoma cell line SH-SY5Y. Hep-G2 cells were cultivated in RPMI1640 (ThermoFisher) supplemented with 10% FBS and SH-SY5Y cells were cultivated in DMEM (high-glucose, pyruvate) (ThermoFisher) also supplemented with 10% FBS in a humidified atmosphere of 37 °C and 5% CO₂ according to standard cell culture procedures. For the assay, cells were plated in 96-well microtiter plates (Greiner bio-one) at densities of 50 000 cells/well (Hep-G2) and 60 000 cells/well (SH-SY5Y), respectively. After 24 h, compounds dissolved in DMSO are added to fresh medium at concentrations of 30 and 100 μ M [final concentration of DMSO: 1% (v/v)] and applied to the cells for another 24 h. On the next day, cellular viability is determined using the CytoTox-ONE kit (Promega) based on the viability in control wells incubated with culture medium and 1% DMSO. In brief, cells were washed two times with PBS. After an incubation with 50 μ L lysis solution (9% w/v of Triton X-100 in water) for 10 min at room temperature following a 10 min incubation with an equal volume of

CytoTox-ONE reagent. A stop solution was applied and fluorescence signals were recorded (544/595 nm) using a CLARIOstar plate reader.

Acknowledgements

We gratefully acknowledge Antje Hamann and Christian Pfennig (IZI-MWT), Dr. Christoph Wiedemann, and Dr. Christian Ihling (Martin Luther University, Halle–Wittenberg) for their excellent technical support.

Disclosure statement

M. B. is an employee of PerioTrap Pharmaceuticals GmbH. C. J. is an employee of Vivoryon Therapeutics N.V., Halle (Saale), Germany. The remaining authors declare no competing interests.

Preprint

A previous version of this manuscript has been deposited as a preprint on ChemRxiv (DOI: 10.26434/chemrxiv-2022-jflzq).

Funding

Parts of this work were supported by grants from European Regional Development Fund (#ZS/2019/02/97143) and from the German Federal Ministry of Education and Research (#16GW0288K).

ORCID

Kathrin Tan  <http://orcid.org/0000-0003-0565-2676>

Christian Jäger  <http://orcid.org/0000-0002-2740-8386>

Stefanie Geissler  <http://orcid.org/0000-0003-3293-3043>

Dagmar Schlenzig  <http://orcid.org/0000-0002-7474-5641>

Mirko Buchholz  <http://orcid.org/0000-0002-2629-4153>

Daniel Ramsbeck  <http://orcid.org/0000-0002-4966-142X>

References

1. Drag M, Salvesen GS. Emerging principles in protease-based drug discovery. *Nat Rev Drug Discov.* 2010;9(9):690–701.
2. Gomis-Rüth FX, Trillo-Muyo S, Stöcker W. Functional and structural insights into astacin metalloproteinases. *Biol Chem.* 2012;393(10):1027–1041.
3. Sterchi EE, Stöcker W, Bond JS. Meprins, membrane-bound and secreted astacin metalloproteinases. *Mol Asp Med.* 2008;29(5):309–328.
4. Scharfenberg F, Armbrust F, Marengo L, Pietrzik C, Becker-Pauly C. Regulation of the alternative β -secretase meprin β by ADAM-mediated shedding. *Cell Mol Life Sci.* 2019;76(16):3193–3206.
5. Peters F, Scharfenberg F, Colmorgen C, Armbrust F, Wichert R, Arnold P, Potempa B, Potempa J, Pietrzik CU, Häslers R, et al. Tethering soluble meprin α in an enzyme complex to the cell surface affects IBD-associated genes. *FASEB J.* 2019;33(6):7490–7504.
6. Broder C, Becker-Pauly C. The metalloproteinases meprin α and meprin β : unique enzymes in inflammation, neurodegeneration, cancer and fibrosis. *Biochem J.* 2013;450(2):253–264.
7. Prox J, Arnold P, Becker-Pauly C. Meprin α and meprin β : procollagen proteinases in health and disease. *Matrix Biol.* 2015;44-46:7–13.
8. Lottaz D, Maurer CA, Hahn D, Büchler MW, Sterchi EE. Nonpolarized secretion of human meprin alpha in colorectal cancer generates an increased proteolytic potential in the stroma. *Cancer Res.* 1999;59(5):1127–1133.
9. Lottaz D, Maurer CA, Noël A, Blacher S, Huguenin M, Nievergelt A, Niggli V, Kern A, Müller S, Seibold F, et al. Enhanced activity of meprin- α , a pro-migratory and pro-angiogenic protease, in colorectal cancer. *PLOS One.* 2011;6(11):e26450.
10. Minder P, Bayha E, Becker-Pauly C, Sterchi EE. Meprin α transactivates the epidermal growth factor receptor (EGFR) via ligand shedding, thereby enhancing colorectal cancer cell proliferation and migration. *J Biol Chem.* 2012;287(42):35201–35211.
11. Wang X, Chen J, Wang J, Yu F, Zhao S, Zhang Y, Tang H, Peng Z. Metalloproteinases meprin- α (MEP1A) is a prognostic biomarker and promotes proliferation and invasion of colorectal cancer. *BMC Cancer.* 2016;16(1):383.
12. OuYang H-Y, Xu J, Luo J, Zou R-H, Chen K, Le Y, Zhang Y-F, Wei W, Guo R-P, Shi M. MEP1A contributes to tumor progression and predicts poor clinical outcome in human hepatocellular carcinoma. *Hepatology.* 2016;63(4):1227–1239.
13. Breig O, Yates M, Neaud V, Couchy G, Grigoletto A, Lucchesi C, Prox J, Zucman-Rossi J, Becker-Pauly C, Rosenbaum J. Metalloproteinase meprin α regulates migration and invasion of human hepatocarcinoma cells and is a mediator of the oncoprotein reptin. *Oncotarget.* 2017;8(5):7839–7851.
14. Grainger AT, Pilar N, Li J, Chen M-H, Abramson AM, Becker-Pauly C, Shi W. Identification of Mep1a as a susceptibility gene for atherosclerosis in mice. *Genetics.* 2021;219(4):iyab160.
15. Ge W, Hou C, Zhang W, Guo X, Gao P, Song X, Gao R, Liu Y, Guo W, Li B, et al. Mep1a contributes to Ang II-induced cardiac remodeling by promoting cardiac hypertrophy, fibrosis and inflammation. *J Mol Cell Cardiol.* 2021;152:52–68.
16. Gao R, Liu D, Guo W, Ge W, Fan T, Li B, Gao P, Liu B, Zheng Y, Wang J. Mep1A enhances TNF-alpha secretion by mast cells and aggravates abdominal aortic aneurysms. *Br J Pharmacol.* 2020;177(12):2872–2885.
17. Schäffler H, Li W, Helm O, Krüger S, Böger C, Peters F, Röcken C, Sebens S, Lucius R, Becker-Pauly C, et al. The cancer-associated meprin β variant G32R provides an additional activation site and promotes cancer cell invasion. *J Cell Sci.* 2019;132(11):jcs220665.
18. Gellrich A, Scharfenberg F, Peters F, Sammel M, Helm O, Armbrust F, Schmidt F, Lokau J, Garbers C, Sebens S, et al. Characterization of the cancer-associated meprin β variants G45R and G89R. *Front Mol Biosci.* 2021;8:702341.
19. Bien J, Jefferson T, Causevic M, Jumpertz T, Munter L, Multhaup G, Weggen S, Becker-Pauly C, Pietrzik CU. The metalloproteinase meprin generates amino terminal-truncated amyloid peptide species. *J Biol Chem.* 2012;287(40):33304–33313.
20. Schönherr C, Bien J, Isbert S, Wichert R, Prox J, Altmeppen H, Kumar S, Walter J, Lichtenthaler SF, Weggen S, et al. Generation of aggregation prone N-terminally truncated amyloid β peptides by meprin β depends on the sequence specificity at the cleavage site. *Mol Neurodegener.* 2016;11(11):19.

21. Becker-Pauly C, Pietrzik CU. The metalloprotease meprin β is an alternative β -secretase of APP. *Front Mol Neurosci*. 2016; 9:159.
22. Armbrust F, Colmorgen C, Pietrzik CU, Becker-Pauly C. The Alzheimer's disease associated bacterial protease RgpB from *P. gingivalis* activates the alternative β -secretase meprin β thereby increasing A β generation. *bioRxiv*. 2019:748814.
23. Berner DK, Wessolowski L, Armbrust F, Schneppenheim J, Schlepckow K, Koudelka T, Scharfenberg F, Lucius R, Tholey A, Kleinberger G, et al. Meprin β cleaves TREM2 and controls its phagocytic activity on macrophages. *FASEB J*. 2020;34(5): 6675–6687.
24. Broder C, Arnold P, Vadon-Le Goff S, Konerding MA, Bahr K, Muller S, Overall CM, Bond JS, Koudelka T, Tholey A, et al. Metalloproteases meprin and meprin are C- and N-procollagen proteinases important for collagen assembly and tensile strength. *Proc Natl Acad Sci USA*. 2013;110(35):14219–14224.
25. Biasin V, Marsh LM, Egemnazarov B, Wilhelm J, Ghanim B, Klepetko W, Wygrecka M, Olschewski H, Eferl R, Olschewski A, et al. Meprin β , a novel mediator of vascular remodelling underlying pulmonary hypertension. *J Pathol*. 2014;233(1):7–17.
26. Biasin V, Wygrecka M, Marsh LM, Becker-Pauly C, Brcic L, Ghanim B, Klepetko W, Olschewski A, Kwapiszewska G. Meprin β contributes to collagen deposition in lung fibrosis. *Sci Rep*. 2017;7:39969.
27. Kruse M-N, Becker C, Lottaz D, Köhler D, Yiallourous I, Krell H-W, Sterchi EE, Stöcker W. Human meprin alpha and beta homo-oligomers: cleavage of basement membrane proteins and sensitivity to metalloprotease inhibitors. *Biochem J*. 2004;378(Pt 2):383–389.
28. Herzog C, Haun RS, Kaushal GP. Role of meprin metalloproteinases in cytokine processing and inflammation. *Cytokine*. 2019;114:18–25.
29. Herzog C, Seth R, Shah SV, Kaushal GP. Role of meprin A in renal tubular epithelial cell injury. *Kidney Int*. 2007;71(10): 1009–1018.
30. Kaushal GP, Haun RS, Herzog C, Shah SV. Meprin A metalloproteinase and its role in acute kidney injury. *Am J Physiol Renal Physiol*. 2013;304(9):F1150–F1158.
31. Herzog C, Marisiddaiah R, Haun RS, Kaushal GP. Basement membrane protein nidogen-1 is a target of meprin β in cisplatin nephrotoxicity. *Toxicol Lett*. 2015;236(2):110–116.
32. Banerjee S, Bond JS. Prointerleukin-18 is activated by meprin beta *in vitro* and *in vivo* in intestinal inflammation. *J Biol Chem*. 2008;283(46):31371–31377.
33. Banerjee S, Jin G, Bradley SG, Matters GL, Gailey RD, Crisman JM, Bond JS. Balance of meprin A and B in mice affects the progression of experimental inflammatory bowel disease. *Am J Physiol Gastrointest Liver Physiol*. 2011;300(2):G273–G282.
34. Vandenbroucke RE, Libert C. Is there new hope for therapeutic matrix metalloproteinase inhibition? *Nat Rev Drug Discov*. 2014;13(12):904–927.
35. Dufour A, Overall CM. Missing the target: matrix metalloproteinase antitargets in inflammation and cancer. *Trends Pharmacol Sci*. 2013;34(4):233–242.
36. Madoux F, Tredup C, Spicer TP, Scampavia L, Chase PS, Hodder PS, Fields GB, Becker-Pauly C, Minond D. Development of high throughput screening assays and pilot screen for inhibitors of metalloproteases meprin α and β . *Biopolymers*. 2014;102(5):396–406.
37. Ramsbeck D, Hamann A, Schlenzig D, Schilling S, Buchholz M. First insight into structure–activity relationships of selective meprin β inhibitors. *Bioorg Med Chem Lett*. 2017; 27(11):2428–2431.
38. Ramsbeck D, Hamann A, Richter G, Schlenzig D, Geissler S, Nykiel V, Cynis H, Schilling S, Buchholz M. Structure-guided design, synthesis, and characterization of next-generation meprin β inhibitors. *J Med Chem*. 2018;61(10):4578–4592.
39. Tan K, Jäger C, Schlenzig D, Schilling S, Buchholz M, Ramsbeck D. Tertiary-amine-based inhibitors of the astacin protease meprin α . *ChemMedChem*. 2018;13(16):1619–1624.
40. Linnert M, Fritz C, Jäger C, Schlenzig D, Ramsbeck D, Kleinschmidt M, Wermann M, Demuth H-U, Parthier C, Schilling S. Structure and dynamics of meprin β in complex with a hydroxamate-based inhibitor. *IJMS*. 2021;22(11):5651.
41. Becker-Pauly C, Barré O, Schilling O, Auf Dem Keller U, Ohler A, Broder C, Schütte A, Kappelhoff R, Stöcker W, Overall CM. Proteomic analyses reveal an acidic prime side specificity for the astacin metalloprotease family reflected by physiological substrates. *Mol Cell Proteomics*. 2011;10(9):M111.009233.
42. Villa JP, Bertenshaw GP, Bond JS. Critical amino acids in the active site of meprin metalloproteinases for substrate and peptide bond specificity. *J Biol Chem*. 2003;278(43):42545–42550.
43. Hou S, Diez J, Wang C, Becker-Pauly C, Fields GB, Bannister T, Spicer TP, Scampavia LD, Minond D. Discovery and optimization of selective inhibitors of meprin α (part I). *Pharmaceuticals*. 2021;14(3):203.
44. Wang C, Diez J, Park H, Spicer TP, Scampavia LD, Becker-Pauly C, Fields GB, Minond D, Bannister TD. Discovery and optimization of selective inhibitors of meprin α (part II). *Pharmaceuticals*. 2021;14(3):197.
45. Tan K, Jäger C, Körschgen H, Geissler S, Schlenzig D, Buchholz M, Stöcker W, Ramsbeck D. Heteroaromatic inhibitors of the astacin proteinases meprin α , meprin β and ovas-tacin discovered by a scaffold-hopping approach. *ChemMedChem*. 2021;16(6):976–988.
46. Heller ST, Natarajan SR. 1,3-diketones from acid chlorides and ketones: a rapid and general one-pot synthesis of pyrazoles. *Org Lett*. 2006;8(13):2675–2678.
47. Riley K, Tran K-A. Strength and character of R–X $\cdots\pi$ interactions involving aromatic amino acid sidechains in protein-ligand complexes derived from crystal structures in the protein data bank. *Crystals*. 2017;7(9):273.
48. Adiguzel E, Yilmaz F, Emirik M, Ozil M. Synthesis and characterization of two new hydroxamic acids derivatives and their metal complexes. An investigation on the keto/enol, E/Z and hydroxamate/hydroximate forms. *J Mol Struct*. 2017; 1127:403–412.
49. Citarella A, Moi D, Pinzi L, Bonanni D, Rastelli G. Hydroxamic acid derivatives: from synthetic strategies to medicinal chemistry applications. *ACS Omega*. 2021;6(34):21843–21849.
50. Jones G, Willett P, Glen RC, Leach AR, Taylor R. Development and validation of a genetic algorithm for flexible docking. *J. Mol. Biol*. 1997;267(3):727–748.
51. Verdonk ML, Cole JC, Hartshorn MJ, Murray CW, Taylor RD. Improved protein-ligand docking using GOLD. *Proteins*. 2003;52(4):609–623.
52. Lovell SC, Word JM, Richardson JS, Richardson DC. The penultimate rotamer library. *Proteins*. 2000;40(3):389–408.
53. Molecular operating environment (MOE), 2019.01. Montreal: Chemical Computing Group ULC; 2019.
54. Schlenzig D, Wermann M, Ramsbeck D, Moenke-Wedler T, Schilling S. Expression, purification and initial

- characterization of human meprin β from *Pichia pastoris*. *Protein Expr Purif.* 2015;116:75–81.
55. Bayly-Jones C, Lupton CJ, Fritz C, Venugopal H, Ramsbeck D, Wermann M, Jäger C, Marco A. d, Schilling S, Schlenzig D. Helical ultrastructure of the metalloprotease meprin α in complex with a small molecule inhibitor. *Nat Commun.* 2022;13(1):6178.
56. Morrison JF. Kinetics of the reversible inhibition of enzyme-catalysed reactions by tight-binding inhibitors. *Biochim Biophys Acta.* 1969;185(2):269–286.